Accepted Manuscript

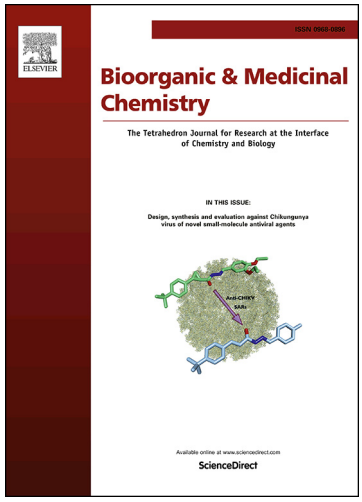

Discovery of 18β-glycyrrhetinic acid conjugated aminobenzothiazole derivatives as Hsp90–Cdc37 interaction disruptors that inhibit cell migration and reverse drug resistance

Le Jin, Rizhen Huang, Xiaochao Huang, Bin Zhang, Min Ji, Hengshan Wang

PII: S0968-0896(17)32426-4
DOI: https://doi.org/10.1016/j.bmc.2018.02.021
Reference: BMC 14207

To appear in: *Bioorganic & Medicinal Chemistry*

Received Date: 14 December 2017
Revised Date: 9 February 2018
Accepted Date: 15 February 2018

Please cite this article as: Jin, L., Huang, R., Huang, X., Zhang, B., Ji, M., Wang, H., Discovery of 18β-glycyrrhetinic acid conjugated aminobenzothiazole derivatives as Hsp90–Cdc37 interaction disruptors that inhibit cell migration and reverse drug resistance, *Bioorganic & Medicinal Chemistry* (2018), doi: https://doi.org/10.1016/j.bmc.2018.02.021

Discovery of 18β-glycyrrhetinic acid conjugated aminobenzothiazole derivatives as Hsp90–Cdc37 interaction disruptors that inhibit cell migration and reverse drug resistance

Le Jin[a, 1], Rizhen Huang[b, 1], Xiaochao Huang[b, 1], Bin Zhang[c], Min Ji[a, *] and Hengshan Wang[c, *]

[a] *School of Biological Science and Medical Engineering, Southeast University, Nanjing 210096, China.*

[b] *Pharmaceutical Research Center and School of Chemistry and Chemical Engineering, Southeast University, Nanjing 211189, China.*

[c] *State Key Laboratory for the Chemistry and Molecular Engineering of Medicinal Resources (Ministry of Education of China), School of Chemistry and Pharmaceutical Sciences of Guangxi Normal University, Guilin 541004, PR China.*

Author information

Corresponding Authors: School of Biological Science and Medical Engineering, Southeast University, Nanjing 210096, China.

*E-mail: jiminseu@163.com

*E-mail: whengshan@163.com

Author contributions

[1] Le Jin, Rizhen Huang and Xiaochao Huang contributed equally to this work.

Abstract

A series of 18β-glycyrrhetinic acid (GA) conjugated aminobenzothiazole derivatives were designed, synthesized and evaluated for disruption activity of Hsp90-Cdc37 as well as the effects of *in vitro* cell migration. These compounds exhibited relatively good disruption activity against Hsp90-Cdc37 with IC_{50} values in low micromolar range. A docking study of the most active compound **11g** revealed key interactions between **11g** and Hsp90-Cdc37 complex in which the benzothiazole moiety and the amine chain group were important for improving activity. It is noteworthy that further antitumor activity screening revealed that some compounds exhibited better inhibitory activity than the commercial anticancer drug 5-FU and showed potent suppression activity against drug-resistant cancer cells. In particular, compound **11g** appeared to be the most potent compound against the A549 cell line, at least partly, by inhibition of the activity of Hsp90 and apoptosis induction. The treatment of A549 cells with compound **11g** resulted in inhibition of *in vitro* cell migration through wound healing assay and S phase of cell cycle arrested. In addition, **11g**-induced apoptosis was significantly facilitated in A549 cells. Thus, we conclude that GA aminobenzothiazole derivatives may be the potential Hsp90-Cdc37 disruptors with the ability to suppress cells migration and reversed drug-resistant.

Keywords: 18β-glycyrrhetinic acid; aminobenzothiazole; Hsp90-Cdc37 interaction; Drug resistance; Migration

1. Introduction

Cancer metastasis and drug resistance have been two major impediments to effective cancer treatment with conventional chemotherapeutic drugs and have been the leading cause of cancer-associated death in several cancers including liver, breast and lung cancers.[1-3] One strategy to address this problem is to identify targets, such as Hsp90,[4] the proteasome,[5] and the autophagosome,[6] that affect multiple signaling pathways or the basic machinery required for cancer cells to survive under stress. As metastasis and clinical drug resistance frequently hinders the treatment of neoplastic disease, extensive research has been carried out.[7] Unfortunately, no useful method for efficient and clinical cancer treatment has been developed, which called for the urgent need for new classes of potent and specific anticancer drugs.

Heat shock protein 90 (Hsp90) is responsible for the conformational maturation, activation, and stability of more than 200 client proteins involved in signal transduction which is essential for oncogenic development, cancer cell survival, and drug resistance development.[8, 9] Hsp90 is continuously overexpressed in cancer cells but not in normal cells and has been demonstrated to be a promising anticancer target with fewer side effects.[10] Therefore, inhibition of Hsp90 is an attractive strategy for the therapeutics of cancers. Many inhibitors targeting Hsp90, including N-terminal Hsp90 inhibitors, C-terminal Hsp90 inhibitors, and non-ATP competitive Hsp90 inhibitors, have been investigated in various clinical settings (**Fig. 1**).[11-15] In addition to the N- or C-terminal Hsp90 inhibitors that bind to the ATP-binding pocket, the non-ATP competitive Hsp90 inhibitors have attracted more and more interest recently and are expected to arrest the chaperone cycle by different mechanisms. It has been proposed that inhibitors targeting the Hsp90−cochaperone or the Hsp90−client complex may be more effective in regulating the function of Hsp90.[16] Cdc37 is a highly specialized cochaperone adaptor in response for for loading kinase client proteins to Hsp90 supercomplex.[17] Hsp90-Cdc37 complex is overexpressed and hyperactivated in many types of tumour cells.[18] Silencing of Cdc37 down-regulates Hsp90 kinase client proteins via a proteasome-mediated degradation pathway, leading to inactivation of multiple downstream signalling pathways and subsequent apoptosis of cancer cells.[19-21] Thus, disruption of the Hsp90-Cdc37 interaction many results in the degradation of the oncogenic kinases and may represent an effective approach for cancer treatment.

Recently, triterpenoids have been identified to be novel non ATP-competitive Hsp90 inhibitors.

[22, 23] Triterpenoids are highly multifunctional and have attracted much attention as potential anticancer agents due to their ability to interact with multiple biological targets. 18β-Glycyrrhetinic acid (GA) served as one of the major effective components of many traditional Chinese medicines has attracted a lot of interest because of its unique anticancer properties.[24, 25] Notably, GA and its derivatives are already known to target various kinases or to act as proteasome inhibitors.[26, 27] However, to the best of our knowledge, the derivatives of GA have not been thoroughly explored for their antitumor activity, especially as the disruptors of Hsp90-Cdc37 interaction. Thus, in order to search potentially important anticancer drug candidates, further study needed to investigate the mechanism of GA based Hsp90-Cdc37 disruptors.

Meanwhile, considerable attention has been also focused on benzothiazoles which have been widely used as functional groups in medicinal chemistry. Research had shown that the incorporation of a benzothiazoles moiety to pharmacy cores could effectively improve the antitumor activity and the cells selectively.[28-30] Interestingly, aminobenzothiazole moiety could induce selective cytotoxicity in developing anti-tumor agents.[31, 32] Moreover, it is reported that the introduction of ester-joined groups at 3-OH of GA could improve the antitumor effect.[33] In view of these findings, aminobenzothiazole group was rationally designed and introduced to the GA structure. These congeners were evaluated for their in vitro anticancer activity and disruption activity of Hsp90-Cdc37. The mode of action of representative compound **11g** that disrupted Hsp90-Cdc37 interaction was also investigated.

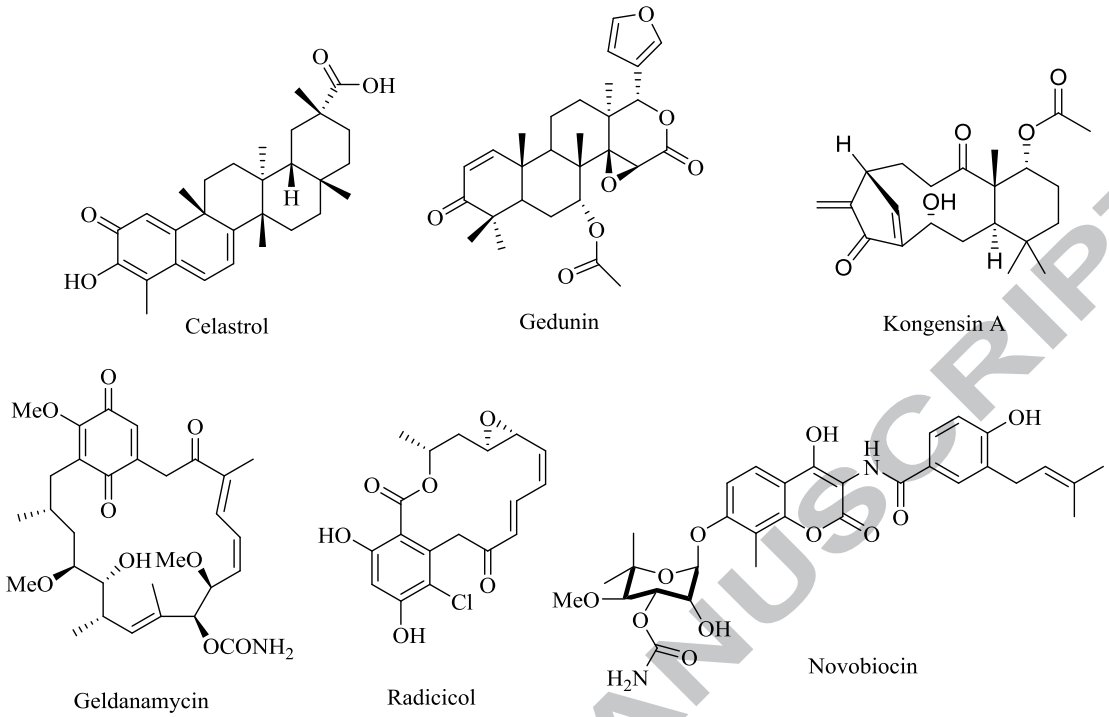

Fig. 1. Chemical structures of Hsp90 inhibitors.

2. Results and discussion

2.1. Chemistry.

The general procedures for the synthesis of glycyrrhetinic acid contained aminobenzothiazole derivatives are shown in Scheme **1**. Aminobenzothiazole derivatives (**2a**-**2k**) were obtained by treating aniline with bromine, acetic acid, and ammonium thiocyanate. GA was acetylated in C-3 with acetic anhydride in pyridine to obtain ester **4**, then **4** followed by its acylation with oxalyl chloride in the presence of dry dichloromethane to obtain the key intermediate **5**. Subsequently, the target compounds **6a**-**6k** were achieved by the formation of amide bond between **5** and **2**, respectively, in the presence of chloroform at reflux. Compound **6** was hydrolyzed by NaOH to afford compounds **7a**-**7k**. GA was acetylated in C-30 with ethyl bromide to obtain **8**. The 3β-hydroxy group of **8** was reacted with succinic anhydride in the presence of 4-dimethylaminopyridine (DMAP) to obtain the target product **9**. The target compounds **11a**-**11k** were synthesized from **9** by the same method as compounds **6a**-**6k**. The structures of target compounds **6a**-**6k**, **7a**-**7k** and **11a**-**11k** were then confirmed by ^{1}H NMR, ^{13}C NMR and high resolution mass spectrometry (HR-MS).

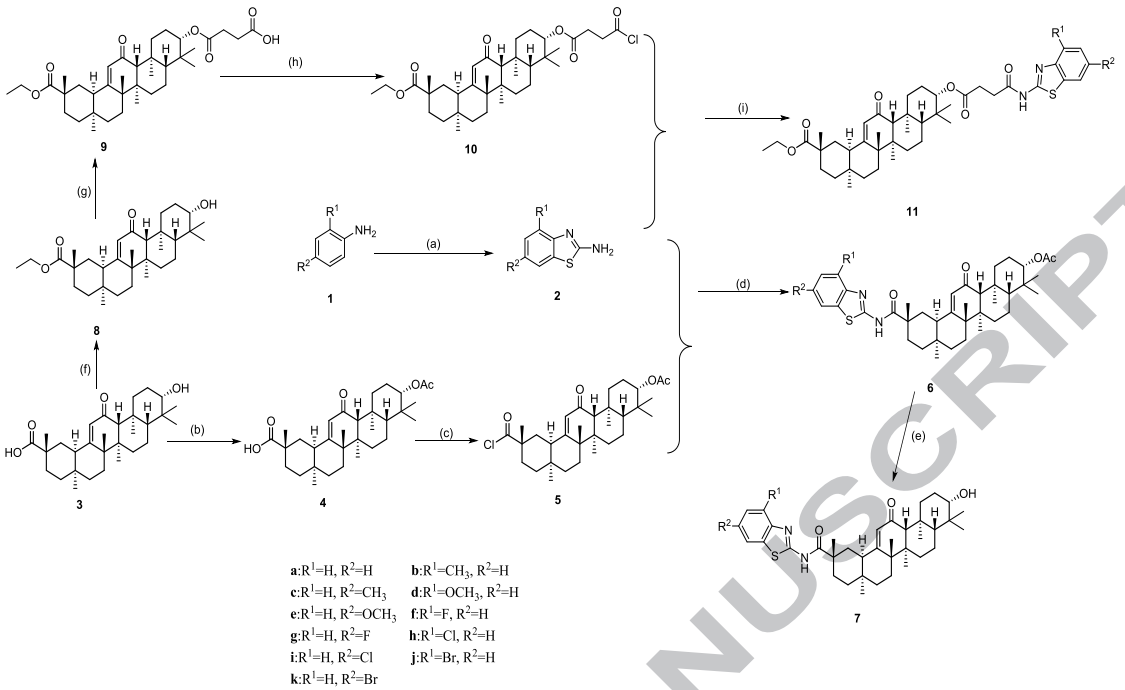

Scheme 1. Synthetic route for the final compounds **6a-6k**, **7a-7k** and **11a-11k** from 18β-glycyrrhetinic acid. Reagents and conditions: (a) aniline, NH_4SCN, glacial acetic acid, 4 h; (b) pyridine, 0 ^oC, 24 h; (c) oxalyl chloride, CH_2Cl_2, 0 ^oC, 12 h; (d) $CHCl_3$, reflux, 5 h; (e) NaOH aq., MeOH/THF, 40 ^oC, 5 h; (f) EtBr, K_2CO_3, acetone, 35 ^oC, 48 h; (g) succinic anhydride, DMAP, CH_2Cl_2, rt, 24 h; (h) oxalyl chloride, CH_2Cl_2, 0 ^oC, 12 h;.(i) $CHCl_3$, reflux, 5 h.

2.2. Biological evaluation.

2.2.1. Hsp90–Cdc37 disruption activities.

The synthesized GA derivatives containing aminobenzothiazole moiety were assayed disruption activity in vitro against Hsp90–Cdc37 interaction using time-resolved fluorescence resonance energy transfer (TR-FRET) according to a previously reported procedure.[34] GA and a novel Hsp90 inhibitor celastrol were taken as positive control. The IC_{50} values obtained in the performed in vitro inhibition assays of GA derivatives are summarized in Table 1.

As shown in Table 1, the newly synthesized GA derivatives are potent Hsp90–Cdc37 inhibitors, with IC_{50} values mostly in micromolar or submicromolar levels. As we can see from Table 1, compound **6**, the acetylated product of compound **7**, substantially decreased Hsp90–Cdc37 disruption activities compared with the un-substituted derivatives **7**, which indicated C-30 position of GA was probably the key interacting fragment upon binding to Hsp90–Cdc37 complex. Notably, all compounds of **11** by introduction the long chain aminobenzothiazole to C-30 position of GA

revealed considerably higher potency than compounds **6** and **7**, suggesting further that the positive contribution of this position to Hsp90–Cdc37 disruption. The results also indicated that the longer chain may be beneficial for inhibition activity. It was established that the position of substituent on benzothiazole moiety as well as the polar significantly affected Hsp90–Cdc37 disruption activities. Among them, the most potent Hsp90–Cdc37 inhibitor, compound **11g** bearing a 5-F moiety, effectively inhibited Hsp90–Cdc37 in the submicromolar range (IC_{50} = 0.14 μM). The effects of the position of substituent showed that the C-5 substitution on benzothiazole generally enhanced Hsp90–Cdc37 disruption, in comparison to a C-7 substitution. Thus, compound **11g** showed the strongest inhibition against Hsp90–Cdc37 in the submicromolar range. In contrast, compound (**11f**), possessing the C-7 substitution scaffold on benzothiazole, was 7.5-fold weaker toward Hsp90–Cdc37 disruption (IC_{50} = 1.05 μM). On the other hand, analysis of the effects of the terminal substituents at the R_1 or R_2 positions of aminobenzothiazole moiety showed that a halogen group generally enhanced Hsp90–Cdc37 inhibition, compared with a methyl or methoxy group substitution. When the methyl of compound **11c** was replaced with a chlorine group at the 5-position on the benzothiazole (compound **11i**), the inhibition potency was markedly increased, and the inhibitory activity was increased 17.8-fold compared with **11c**. More, there was a remarkable increase in potency when replacing the 7-position on the phenyl ring with a chlorine or fluorine group to yield compounds **11f** and **11h** separately, demonstrating that the electron-withdrawing substituents may play a critical role in potent disruption activities against Hsp90–Cdc37.

Table 1

Hsp90–Cdc37 disruption activities and antiproliferative activities of GA and its derivatives **6, 7** and **11**.

		antiproliferative activities IC_{50} (μM)			
Compd.	IC_{50} (μM)	A549	MCF-7	HepG2	Hct-116
6a	>100	>100	>100	>100	>100
6b	>100	>100	>100	>100	>100
6c	>100	>100	>100	>100	>100
6d	>100	>100	>100	>100	>100
6e	90.07±0.91	75.45±1.56	81.16±2.38	85.61±3.05	>100
6f	>100	>100	>100	>100	>100
6g	54.33±0.69	85.45±2.36	71.16±2.28	65.61±2.15	>100
6h	>100	>100	>100	>100	>100
6i	77.58±0.51	62.62±3.09	66.67±2.81	73.12±2.71	68.48±2.79
6j	>100	>100	>100	>100	>100

6k	81.92±0.43	69.69±1.53	78.08±2.77	85.97±3.28	76.75±2.63
7a	89.5±0.67	75.37±1.49	71.37±1.92	87.99±2.86	80.69±2.29
7b	>100	>100	>100	>100	>100
7c	83.16±0.69	22.40±1.82	23.19±1.45	27.55±2.58	18.74±2.43
7d	>100	75.96±1.71	74.50±3.09	86.34±2.92	74.72±3.16
7e	62.38±0.16	51.11±2.91	52.67±2.31	60.12±3.17	54.21±1.62
7f	45.72±0.36	36.45±2.56	41.16±2.68	45.61±3.35	42.50±2.88
7g	32.34±0.88	32.17±2.45	31.12±1.64	36.44±2.43	31.54±2.73
7h	65.63±0.93	75.35±1.53	71.16±2.58	69.60±3.35	>100
7i	36.87±0.47	22.81±1.16	16.52±1.22	21.76±1.59	16.34±1.61
7j	>100	>100	>100	>100	>100
7k	41.30±0.72	33.36±0.78	33.82±2.35	39.49±0.96	37.35±2.07
11a	9.09±0.24	18.81±1.16	20.52±1.22	25.76±1.59	22.34±1.61
11b	21.85±0.15	22.81±1.16	26.52±1.22	31.76±1.59	26.34±1.61
11c	14.87±0.11	19.09±1.35	22.48±1.17	27.51±1.34	23.58±1.06
11d	10.36±0.23	16.36±0.84	20.09±0.63	21.87±1.36	23.11±1.41
11e	8.24±0.38	15.48±0.92	18.54±0.59	20.45±1.65	21.26±1.32
11f	1.05±0.11	9.07±0.68	10.91±1.46	12.52±1.17	10.06±1.53
11g	0.14±0.03	4.04±0.66	6.37±0.82	10.56±1.03	7.97±0.47
11h	1.67±0.12	13.57±0.79	15.01±1.05	16.98±0.89	15.36±1.08
11i	0.83±0.08	6.09±1.12	8.66±0.79	12.41±1.43	10.95±0.81
11j	15.26±0.42	20.66±1.37	24.45±1.29	29.93±0.60	26.77±1.59
11k	5.07±0.54	14.25±0.79	16.08±0.93	19.04±1.16	15.89±1.18
GA	78.39±0.81	84.25±1.09	74.75±1.77	94.45±1.73	91.25±1.29
Celastrol	6.22±0.37	6.59 ± 0.44	6.84 ± 0.52	6.17 ± 1.03	5.26 ± 1.15
5-FU	-	19.52±0.58	15.78±1.87	23.60±2.11	17.25±1.98

2.2.2. Molecular docking.

To understand the disruption of the most active compound **11g** on the target of Hsp90–Cdc37 complex, we performed molecular docking calculations on the active site of Hsp90–Cdc37 using SYBYL-X 2.0 software and the results are summarized in **Fig. 2** and Table 2. The binding mode of compound **11g** (docking score 10.08), with the best docking score and interaction in the binding site of Hsp90–Cdc37 complex, is described and shown in **Fig. 2**. Some key residues, such as ARG166, LEU34, PHE124, HIS211 and THR171, as well as hydrogen bonds between the selected compound and the residues are also labeled. As shown in **Fig. 2**, compound **11g** was stabilized predominantly by formation a tight network of hydrogen bonds with residues ARG166, LEU34, and PHE124. The carbonyl of the chain moiety, which was important for the Hsp90–Cdc37 disruption activity, formed two hydrogen-bonds with the residues ASN37 and PHE124 of the

active site. Furthermore, the benzothiazole moiety as an acceptor established one hydrogen bond with ASN37 and anchored deeply into the binding pocket as an acceptor, which confirmed that this moiety was also crucial for binding. In addition, the carbonyl of acetyl ester moiety formed two hydrogen bonds with the polar hydrogen of ARG166. The GA skeleton was incompletely occupied by hydrophobic residues consisting of ALA38, GLY121, ASP40, ARG167 and TRP168.

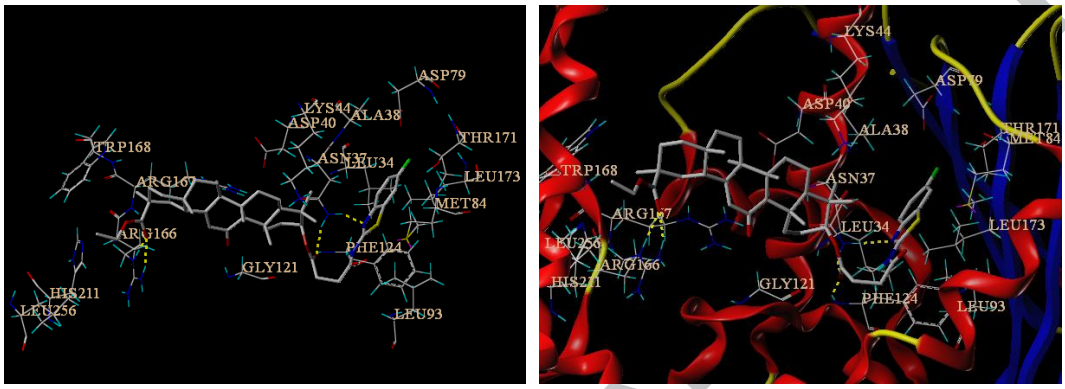

Fig. 2. Binding modes of compound **11g** in the active site of 1US7. Ligands and the important residues for binding interactions are represented by stick and line models. The hydrogen bonds are shown as yellow dotted lines (color figure online).

Table 2

Docking scores (kcal/mol) for all studied compounds

Comd.	Total score	Crash	Polar	D_score	PMF_score	G_score	Chem score	Cscore
6a	3.68	-2.20	0.00	-125.64	-3.07	-282.99	-17.88	3
6b	4.01	-3.29	0.01	-141.07	4.54	-300.61	-22.78	4
6c	4.23	-2.55	1.06	-128.89	-9.68	-255.17	-19.11	4
6d	3.89	-1.72	0.09	-133.63	4.34	-271.22	-22.92	3
6e	4.48	-2.82	0.01	-153.96	11.62	-276.21	-20.37	4
6f	4.41	-2.20	4.01	-117.16	-18.78	-243.60	-16.70	5
6g	6.01	-2.55	1.89	-113.97	-35.32	-239.85	-12.26	2
6h	4.22	-2.16	1.09	-178.66	-11.53	-244.01	-18.58	3
6i	5.35	-2.56	0.02	-205.29	-21.17	-277.26	-19.39	5
6j	3.83	-1.38	0.68	-188.10	-52.43	-240.62	-22.82	4
6k	4.93	-2.16	0.95	-189.46	-29.99	-283.71	-15.95	4
7a	4.45	-1.68	2.33	-127.88	1.66	-272.92	-23.71	4
7b	4.42	-2.35	0.22	-138.38	-14.14	-292.45	-20.70	4
7c	4.87	-1.54	2.34	-129.53	-3.01	-274.88	-24.01	5
7d	3.99	-1.60	1.77	-141.14	-0.92	-297.08	-23.90	4
7e	5.97	-2.84	0.92	-157.53	-13.33	-308.57	-26.50	5
7f	6.10	-1.47	1.74	-128.97	-3.60	-259.59	-21.18	4
7g	6.82	-1.77	1.76	-129.46	8.68	-261.54	-21.34	4
7h	5.06	-2.14	1.81	-231.01	6.77	-273.33	-24.77	3

7i	6.70	-1.89	0.66	-221.64	-10.19	-239.76	-21.18	5
7j	4.08	-1.39	1.66	-194.43	-0.23	-258.15	-23.55	4
7k	6.29	-1.45	1.77	-221.83	-0.51	-258.38	-23.91	4
11a	7.55	-3.54	0.85	-141.72	24.64	-297.38	-18.25	4
11b	6.57	-1.47	2.48	-141.18	-19.03	-295.59	-21.14	3
11c	7.14	-2.39	1.56	-170.01	-14.12	-343.57	-17.17	3
11d	7.05	-2.21	3.99	-176.41	-52.55	-334.75	-23.44	5
11e	7.22	-1.87	2.25	-146.82	-24.74	-268.48	-20.47	2
11f	8.33	-2.55	2.30	-146.69	-13.88	-321.18	-22.99	4
11g	10.08	-2.10	3.14	-167.30	-22.50	-350.12	-28.85	5
11h	8.17	-2.56	2.49	-248.81	-15.11	-338.29	-19.75	4
11i	9.84	-2.22	3.03	-298.95	-29.01	-365.32	-31.09	5
11j	7.12	-1.91	3.46	-152.24	-16.99	-298.00	-21.73	3
11k	7.88	-2.62	2.11	-245.72	-16.69	-296.96	-27.32	4
GA	5.83	-1.04	2.41	-96.743	16.36	-223.06	-18.98	2

2.2.3. Cytotoxicity test.

GA has been reported to show potent anti-proliferative activities against various cancer cell lines.[35] The *in vitro* cytotoxicity of GA and the synthesized target compounds **6**, **7** and **11** were evaluated by MTT assay in a panel of four human cancer cell lines including A549 (lung), HepG2 (hepatoma), MCF-7 (breast) and Hct-116 (colon). The commercial anticancer drugs 5-fluorouracil (5-FU) was served as positive control. The assay results are shown in Table 1.

As shown in Table 1, the IC_{50} values of the most derivatives were lower than that of GA and 5-FU, indicating that the introduction of an aminobenzothiazole moiety in the GA skeleton could improve cytotoxicity. The derivatives **6** and **7** with aminobenzothiazole groups on the carboxyl possessed retained cancer cell growth inhibition activities compared to GA. Derivatives **11** with aminobenzothiazole and longer chain groups on the hydroxy showed more potent anti-proliferative activities, indicating substituents at this position were favorable for the cellular activities. Moreover, compounds **11f-11i** displayed better antitumor activity against the tested cancer cells, suggested the importance of introduction of polar groups as an electron acceptor group at 5 or 7-position for biological activity. However, it was observed that the introduction of hydrophobic (such as methyl and methoxy) substituents in aminobenzothiazole moiety (compounds **11b-11e)** leaded to the decrease of potency against all the tested cancer cell lines. The derivative **11g** with the most potent Hsp90–Cdc37 disruption activity also exhibited the best potent anti-proliferative activities.

2.2.4. Effects of selected compounds on drug resistant cell lines.

It is well-known that Hsp90 inhibitors were reported to be effective against various drug resistant cancer cells.[36] According to the above biological results, we further evaluated the sensitivity of the selected compounds to doxorubicin (DOX) resistant and nonresistant cancer cells (NCI-H460/DOX), with DOX as the positive control. As shown in Table 3, DOX exhibited weaker activity than selected compounds against NCI-H460/DOX resistant cell line. Interestingly, the activity of compounds **11g** and **11i** was not markedly changed for the DOX resistant cancer cell line compared with the sensitive ones and their IC_{50} values of **11g** and **11i** against DOX resistant NCI-H460 cell line were 7.41 and 10.09 μM, respectively. It was significant to observe that compound **11i** had the lowest resistance factor (1.13 for resistant NCI-H460 cell line). Moreover, all of the selected compounds not only exhibited potent cytotoxicity against parental cells and the corresponding DOX resistant cells comparable to that of DOX, but also possessed smaller resistance factors than DOX against DOX-resistant cells. In short, it could be speculated that these compounds might be useful in the treatment of drug refractory tumors resistant to DOX.

Table 3

Cytotoxic effects of selected compounds on NCI-H460/DOX cells line.

Compd.	IC_{50} (μM) [b]		
	NCI-H460	NCI-H460/DOX	R F [c]
11a	16.45±1.65	19.22±1.81	1.17
11f	12.52±2.07	15.36±1.47	1.23
11g	7.41±1.43	10.09±1.33	1.36
11h	13.98±0.89	18.05±1.29	1.29
11i	10.56±1.03	11.97±1.71	1.13
DOX [a]	5.18 ± 1.75	37.95±1.36	7.33

[a] Doxorubicin. [b] IC_{50} values are presented as the mean ± SD (standard error of the mean) from five separated experiments. [c] RF = resistant factor.

*2.2.5 Disruption effect of **11g** on Hsp90-Cdc37complex.*

In order to investigate the disruption of Hsp90-Cdc37 interaction with compound **11g** in A549 cells, thus, we have further used western blot analysis of Cdc37 after immunoprecipitation of

Hsp90. The positive drug geldanamycin was acted as positive control. As shown in **Fig. 3**, immunoprecipitation of Hsp90 pulled down Cdc37 as detected by Western blot, which suggested that Hsp90-Cdc37 formed a complex. The target compound **11g** significantly down-regulated the amount of Cdc37 in the immunoprecipitated Hsp90 complex after cells treated with **11g** at the indicated concentrations (5 and 10 μM), while GDA (10 μM) did not obvious change the level of Cdc37 in immunoprecipitated Hsp90 complex (**Fig. 3**). Moreover, similar to the Hsp90 inhibitor geldanamycin, **11g** induced the up-regulation of Hsp90α and Hsp90β (**Fig. 4**). In short, these results indicated that **11g** acted differently from geldanamycin by inhibiting Hsp90 through disruption of the Hsp90-Cdc37complex.

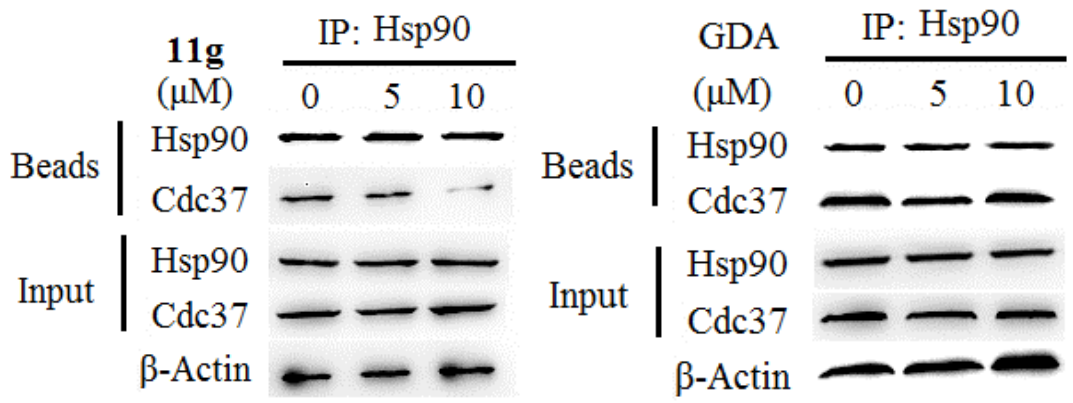

Fig. 3. Compound **11g** disrupts the Hsp90-Cdc37 interaction in lung cancer cells compared with geldanamycin (GDA). A549 cells were treated with compound **11g** or GDA for 24 h. Hsp90 was immunoprecipitated from whole-cell lysates with an anti-Hsp90 antibody, then analyzed by Western blot with antibody against Cdc37 and Hsp90. An equal aliquot of input Hsp90 and Cdc37 were measured by Western blot analysis.

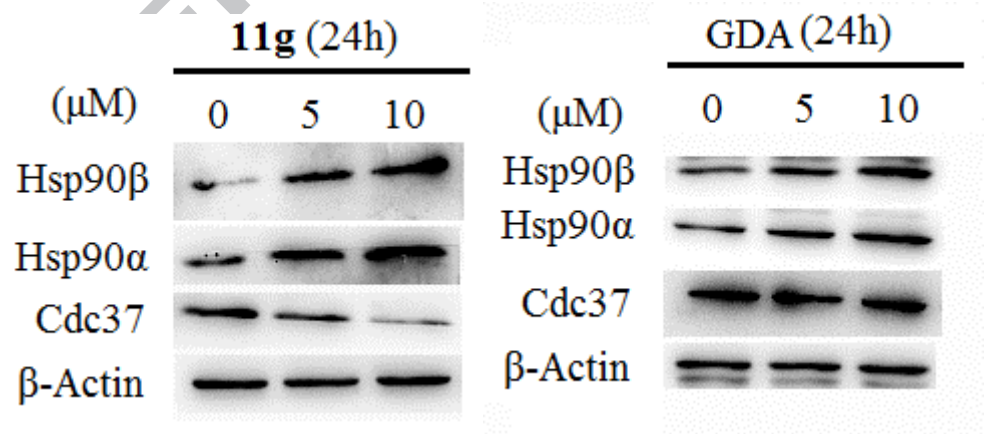

Fig. 4. Effect of **11g** on A549 cells was compared with geldanamycin (GDA). A549 cells were exposed to **11g** or GDA for 24 h, and then whole-cell lysates were subjected to SDSPAGE followed by Western blot analysis of specified proteins. β-Actin was shown as a loading control.

*2.2.6. Effects of **11g** on Hsp90 client proteins*

To clarify the correlation between the anti-proliferative activity and Hsp90 inhibitory activity of

11g, we examined the ability of **11g** to inhibit Hsp90 in the human lung cancer cell line A549. A decrease in Hsp90 client proteins and a compensatory increase in HSPs are the two most common biomarkers used for the inhibition of Hsp90 in cells. In **Fig. 5**, the down-regulation of Hsp90 client proteins including pAkt and CDK4 and the compensatory induction of Hsp70 and Hsp27 in a dose-dependent manner were observed simultaneously as expected, demonstrating that **11g** was an effective Hsp90 inhibitor. These results confirmed that the effects of **11g** on cell proliferation were a consequence of Hsp90 function inhibition.

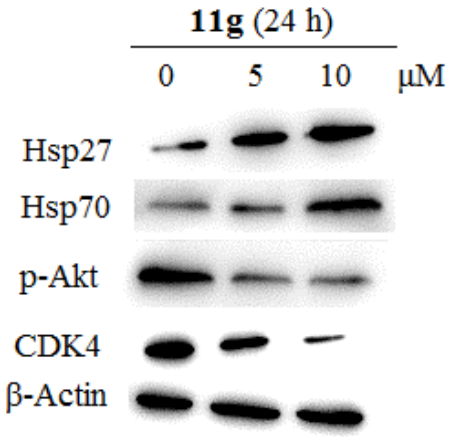

Fig. 5. Western blot analysis of biomarkers modulation of derivatives **11g** in A549 cells at the indicated concentrations and for the indicated times. β-Actin antibody was used as reference control.

*2.2.7. Compound **11g** inhibited the migration of A549 cell in vitro.*

Migration of cells is a key attribute of practically each biological process, which is known to be associated with the tumor progression and metastatic cascade in cancer cells.[37] So the inhibition of metastasis is vital for efficient cancer treatment. Moreover, it has been reported that Hsp90 inhibitors are able to inhibit cancer cell growth and migration.[38] In light of this, we investigated the effect of compound **11g** on cell migration via wound healing assay in A549 cells. The migration of A549 cells was recorded by microscopic observations for 24 h after the treatment with 5 μM and 10 μM of compound **11g**. It was clearly showed that the wound was almost healed completely in the control group after 24 h (**Fig. 6**). However, the process of wound healing was strongly suppressed in the cells when treated with **11g.**

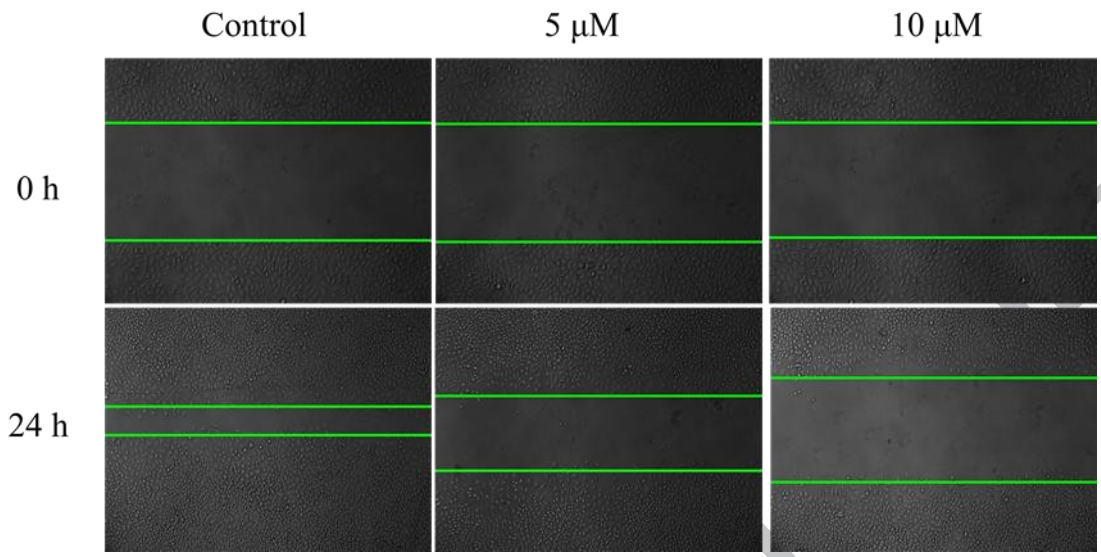

Fig. 6. In vitro cell migration assay. A549 cells were treated with compound **11g** (5 μM and 10 μM) and artificial scratches were done with sterile 200 mL pipette. The images were captured by using a Nikon Te2000 deconvolution microscope (magnification 200×) at 0 h and 24 h.

2.2.8. Cell cycle analysis.

In order to confirm the possible role of cell cycle arrest in GA derivative induced growth inhibition, flow cytometric analysis was carried out to investigate the effects of compound **11g** on the cycle distribution in A549 cells. A549 cells were treated under different concentrations of **11g** for 48 h, with untreated cells as the negative control. As depicted **in Fig. 7**, when treated with compound **11g** at 5 and 10 μM for 48 h, the percentage of G1 phases decrease from 70.16% (the negative control) to 52.92% and 47.14%, respectively. In addition, the percentages of cells in the S phases increased to 34.09% and 40.35% compared with the control (19.62%) under the same conditions. In short, these results indicated that target compound **11g** mainly arrested A549 cells at S phase in a dose-dependent manner.

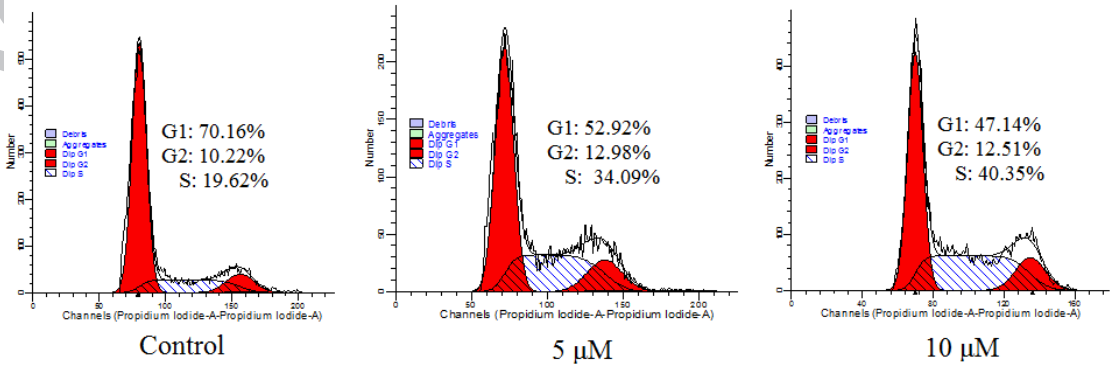

Fig. 7. Compound **11g** induced cell cycle arrest at S phase. A549 cells were treated with 5 or 10 μM compound **11g** for 48 h. Cells were fixed, stained with propidium iodide (PI), and were assessed by flow cytometry. Cells untreated were used for comparison.

*2.2.9. Compound **11g** induced apoptosis in A549 cells.*

The A549 cells apoptosis ratios induced by compound **11g** were quantitatively detected by flow cytometry. The tested compound **11g** was incubated with A549 cells for 24 h at the increasing concentrations and cells were co-stained with annexin-V FITC and PI. Untreated A549 cells were served as a negative control. Quadrants of Q1, Q2, Q3 and Q4 represented four different cell states: necrotic cells, late apoptotic or necrotic cells, living cells, and apoptotic cells, respectively (**Fig. 8**). As shown in **Fig. 8**, a small number of apoptotic A549 cells (0.11%) were presented in the control, while the apoptosis ratio rose to 12.29% and 20.07% after the A549 cells were treated with compound **11g** at different concentrations (5 and 10 μM), respectively. In brief, these results suggested that target compound **11g** could effectively induced apoptosis in A549 cells in a concentration-dependent manner.

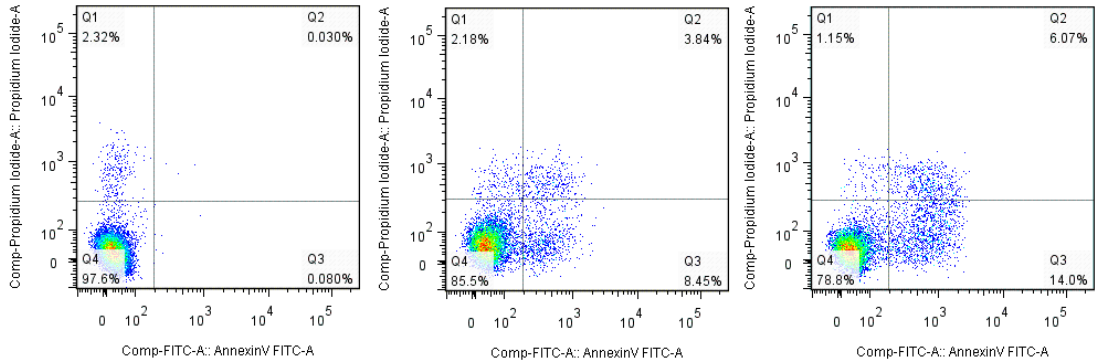

Fig. 8. Annexin V-FITC and PI staining to evaluate apoptosis in A549 cells following compound **11g** treatment. A549 cells were treated with **11g** (5 and 10 μM, for 24 h), incubated with annexin V-FITC and PI and analyzed using flow cytometry.

2.2.10. Morphological characterization of A549 cell apoptosis by Hoechst 33258.

In order to further validate cell apoptosis following treatment with compound **11g**, A549 cells treated with compound **11g** at 5 and 10 μM for 24 h were stained with Hoechst 33258. The observations showed that control cells exhibited weak blue fluorescence in the control group. After the treatment with compound **11g**, some cells emitted brilliant blue fluorescence, and the nuclei of A549 cells appeared hyper-condensed (brightly stained). The number of apoptotic nuclei containing condensed chromatin increased significantly when A549 cells were treated with compound **11g** (10 μM) for 24 h, indicating that apoptosis of A549 cells was induced by compound **11g** in a dose-dependent manner (**Fig. 9**).

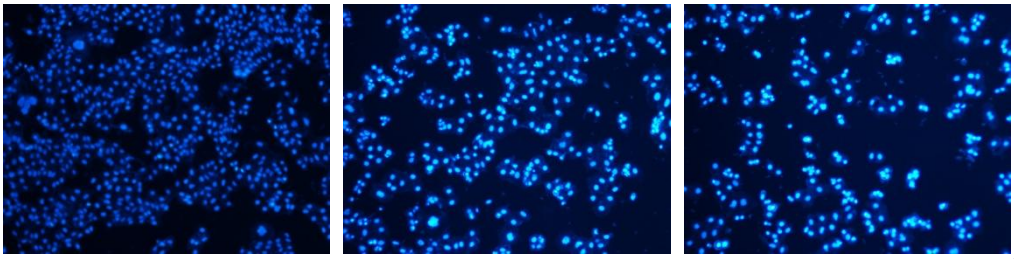

Control 5 μM 10 μM

Fig. 9. Compound **11g** induced apoptotic in A549 cells were determined by Hoechst 33258 staining and were photographed via fluorescence microscopy. A549 cells were treated with **11g** (5 and 10 μM, for 24 h), incubated with Hoechst 33258. Images were acquired using a Nikon Te2000 deconvolution microscope (magnification 200×).

*2.2.11. Compound **11g** triggered ROS generation.*

ROS generations are closely related to mitochondrial depolarization and play a vital role in the progression of apoptosis.[39, 40] Thus, to further investigate the role of ROS production in **11g**-induced apoptotic death in A549 cells, we used the fluorescent probe DCF-DA to detect ROS in cells by flow cytometry. A549 cells were treated with compound **11g** (5 and 10 μM) for 24 h and untreated cells were used as the negative control. As shown in **Fig. 10**, the cells treated with **11g** exhibited the increase of ROS generation in a dose-dependent manner compared with control. Therefore, it was found that **11g** could cause oxidative imbalance in A549 cells.

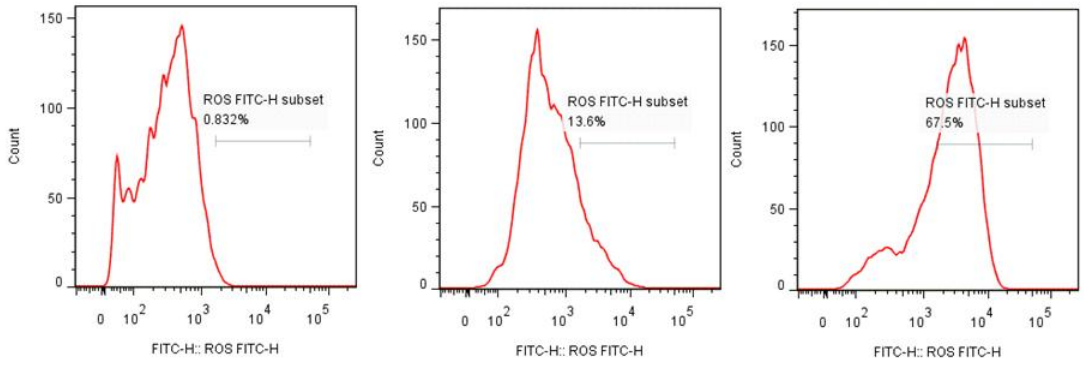

Fig. 10. Compound **11g** affected the levels of intracellular ROS in A549 cells. A549 cells treated with compound **11g** at 5 and 10 μM for 24 h, respectively, detected by flow cytometry. The values represent mean ± S.D. of three independent experiments ($p<0.05$).

*2.2.12. Effects of compound **11g** on the expression of apoptosis-related protein.*

Previously, many studies suggested that the Bcl-2 family proteins have been described as key regulators of MMP.[41, 42] In recent years, a lot of literatures have confirmed that natural products and its derivatives induced mitochondria mediated apoptosis in cancer cells through regulation of Bcl-2 family members.[43-46] Thus, the expression of apoptosis-related proteins was also

investigated. In the present study, western blot analysis displayed that compound **11g** up-regulated the expression of pro-apoptotic proteins (e.g., Bax) and correspondingly down-regulated the expression of anti-apoptotic proteins (e.g., Bcl-2) in a dose-dependent manner (**Fig. 11**), respectively. In addition, caspase proteins such as caspase-3 and caspase-9 are at the core of apoptotic machinery, and play an important role in the execution of apoptosis. Therefore, we further analyzed the ability of compound **11g** to modulate caspase-3 and caspase-9 activities. Further evidence from the Western blot assay demonstrated that compound **11g** effectively up-regulated the expression of cleaved-caspase-3 and cleaved-caspase-9 in a concentration-dependent manner.

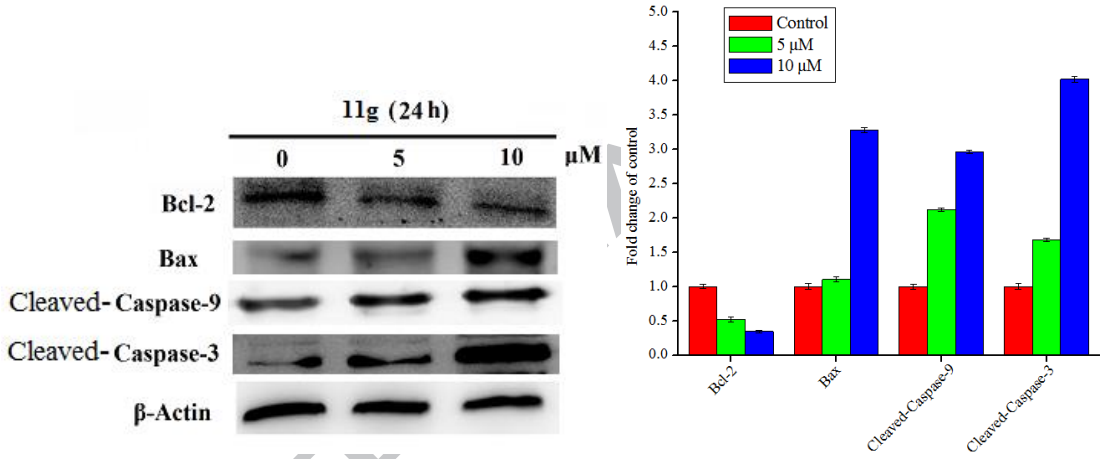

Fig. 11. Western blot analysis of Bcl-2, Bax, cleaved-caspase-9 and cleaved-caspase-3 after treatment of A549 cells with compound **11g** at the indicated concentrations and for the indicated times. β-Actin antibody was used as reference control. Data are expressed as the mean ± S.D. of three independent experiments, $P < 0.05$.

3. Conclusions

A series of GA derivatives containing aminobenzothiazole moiety were designed and synthesized as Hsp90-Cdc37 disruptors with the ability to inhibit migration and drug-resistance. These compounds exhibited significant Hsp90–Cdc37 disruption activities with IC_{50} values at micromolar concentrations. Among them, **11g** exhibited the most potent activity with an IC_{50} value of 0.14 ± 0.02 μM. A docking study of the most active compound **11g** revealed key interactions between **11g** and Hsp90–Cdc37 complex in which the small bulky and strongly electrophilic group of aminobenzothiazole side chain at C-30 positions were important for improving activity. Notably, further antitumor activity screening revealed that some compounds exhibited better inhibitory activity than parent compound UA and commercial anticancer drug 5-FU. Moreover, the selected compounds markedly reversed multidrug-resistance in

DOX-resistant cancer cells. Simultaneous Western blotting analysis showed **11g** could induce the degradation of clients p-Akt and CDK4 dose dependently, suggesting that **11g** exerted its antitumor activities through Hsp90 inhibition in part. Furthermore, cell cycle analysis indicated that compound **11g** arrested the A549 cell line in S phase and induced apoptosis through the mitochondria-mediated pathway. In conclusion, the rational design of aminobenzothiazole GA derivatives offers significant potential for the discovery of a new class of Hsp90 inhibitors with the ability to suppress migration and reverse multidrug resistance in A549 lung cancer cell line.

4. Experimental section

4.1. General information.

All chemicals (reagent grade) used were purchased from Aldrich (U.S.A) and Sinopharm Chemical Reagent Co., Ltd (China). Separation of the compounds by column chromatography was carried out with silica gel 60 (200–300 mesh ASTM, E. Merck).The quantity of silica gel used was 30–70 times the weight charged on the column. Then, the eluates were monitored using TLC (thin-layer chromatography). ESI mass spectra were obtained on a Mariner System 5304 mass spectrometer, and ^{1}H NMR and ^{13}C NMR spectra were recorded on Bruker AV-300 or 500 spectrometer with chemical shifts reported as ppm (in $CDCl_3$, TMS as the internal standard).

4.2. Experimental section

*4.2.1. General procedure for preparation of compounds **2a-2k***

A mixture of aniline (0.05 mol) and NH_4SCN (19.03 g, 0.25 mol) in glacial acetic acid (100 mL) was cooled to 10 ^{o}C in an ice bath and stirred for 10-20 min. Then bromine (2.82 mL, 0.055 mol) in glacial acetic acid was added drop wise at such a rate to keep the temperature below 10 ^{o}C. The mixture was stirred at room temperature for 4 h and then poured into hot water (500 mL), and basified to pH 11.0 with ammonia solution (NH_4OH). The resulting precipitate was filtered, washed with water and dried to get a light yellow to brown solid. The crude product was purified by chromatography on silica gel using MeOH/CH_2Cl_2 to afford compounds **2a-2k** in good yields.

*2-Aminobenzothiazole (**2a**).* This was obtained as a light yellow solid (5.40 g, 72%). ^{1}H NMR (300 MHz, $CDCl_3$) δ 7.65 – 7.47 (m, 2H), 7.30 (t, *J* = 7.5 Hz, 1H), 7.12 (t, *J* = 7.4 Hz, 1H), 5.58 (s, 2H, NH_2).

*2-Amino-4-methylbenzothiazole (**2b**).* This was obtained as a light yellow solid (5.82 g, 71%). ^{1}H NMR (300 MHz, $CDCl_3$) δ 7.43 (d, *J* = 7.7 Hz, 1H), 7.12 (d, *J* = 7.3 Hz, 1H), 7.03 (t, *J* = 7.6 Hz, 1H), 5.67 (s, 2H, NH_2), 2.55 (s, 3H, CH_3).

*2-Amino-6-methylbenzothiazole (**2c**).* This was obtained as a light yellow solid (5.74 g, 71%). ^{1}H NMR (300 MHz, $CDCl_3$) δ 7.45 – 7.36 (m, 2H), 7.11 (d, *J* = 8.1 Hz, 1H), 5.28 (s, 2H, NH_2), 2.39 (s, 3H, CH_3).

*2-Amino-4-methoxybenzothiazole (**2d**).* This was obtained as a light yellow solid (6.66 g, 74%). ^{1}H NMR (300 MHz, $CDCl_3$) δ 7.04 – 6.99 (m, 1H), 6.96 (d, *J* = 1.9 Hz, 1H), 6.67 (d, *J* = 8.1 Hz, 1H), 4.08 (s, 2H, NH_2), 3.88 (s, 3H, OCH_3).

*2-Amino-6-methoxybenzothiazole (**2e**).* This was obtained as a light yellow solid (7.20 g, 80%). ^{1}H NMR (300 MHz, $CDCl_3$) δ 7.44 (d, *J* = 8.8 Hz, 1H), 7.13 (d, *J* = 1.9 Hz, 1H), 6.95 – 6.86 (m, 1H), 5.22 (s, 2H, NH_2), 3.82 (s, 3H, OCH_3).

*2-Amino-4-fluorobenzothiazole (**2f**).* This was obtained as a light yellow solid (6.13 g, 73%). ^{1}H NMR (300 MHz, $CDCl_3$) δ 7.37 – 7.31 (m, 1H), 7.08 – 6.99 (m, 2H), 6.40 (s, 2H, NH_2).

*2-Amino-6-fluorobenzothiazole (**2g**).* This was obtained as a light yellow solid (6.30 g, 75%). ^{1}H NMR (300 MHz, $CDCl_3$) δ 7.37 – 7.24 (m, 2H), 7.04 (s, 2H, NH_2), 6.98 – 6.90 (m, 1H).

*2-Amino-4-chlorobenzothiazole (**2h**).* This was obtained as a light yellow solid (6.31 g, 69%). ^{1}H NMR (300 MHz, $CDCl_3$) δ 7.52 (d, *J* = 2.2 Hz, 1H), 7.33 – 7.28 (m, 1H), 6.79 (d, *J* = 8.5 Hz, 1H), 4.40 (s, 2H, NH_2).

*2-Amino-6-chlorobenzothiazole (**2i**).* This was obtained as a light yellow solid (6.13 g, 67%). ^{1}H NMR (300 MHz, $CDCl_3$) δ 7.52 (s, 1H), 7.31 (d, *J* = 8.4 Hz, 1H), 7.16 (d, *J* = 8.3 Hz, 1H), 7.05 (s, 2H, NH_2).

*2-Amino-4-bromobenzothiazole (**2j**).* This was obtained as a light yellow solid (8.74 g, 77%). ^{1}H NMR (300 MHz, $CDCl_3$) δ 7.50 (d, *J* = 7.7 Hz, 1H), 7.42 (s, 1H), 7.37 (s, 2H, NH_2), 6.91 (t, *J* = 7.8 Hz, 1H).

*2-Amino-6-bromobenzothiazole (**2k**).* This was obtained as a light yellow solid (8.51 g, 77%). ^{1}H NMR (300 MHz, $CDCl_3$) δ 7.67 (s, 1H), 7.33 (d, *J* = 10.2 Hz, 2H), 6.93 (s, 2H, NH_2).

*4.2.2. General procedure for preparation of compound **4**.*

Acetic anhydride (5.0 mL) was added dropwise to a stirred solution of GA (500 mg, 1.06 mmol) in pyridine (7.5 mL) at 0 ^{o}C. The resulting solution was stirred at the room temperature for 24 h

and monitored by TLC. After completion of reaction, the solvent was removed under the reduced pressure. Then the crude was diluted with CH_2Cl_2 (150 mL), washed with water (100 mL) and the organic phase dried over anhydrous Na_2SO_4 and concentrated under reduced pressure to obtain the target product compound **4** (515 mg, 95%) as the white solid precipitate. ^{1}H NMR (300 MHz, $CDCl_3$) δ 5.72 (s, 1H), 4.52 (dd, *J* = 11.3, 4.9 Hz, 1H), 2.80 (d, *J* = 13.5 Hz, 1H), 2.37 (s, 1H), 2.20 (dd, *J* = 13.5, 2.8 Hz, 1H), 2.05 (s, 3H, CH_3), 2.03 – 1.79 (m, 4H), 1.77 – 1.51 (m, 6H), 1.50 – 1.39 (m, 4H), 1.37 (s, 3H, CH_3), 1.34 – 1.25 (m, 2H), 1.23 (s, 3H, CH_3), 1.15 (d, *J* = 10.9 Hz, 6H, 2× CH_3), 1.08 – 0.98 (m, 2H), 0.88 (s, 6H, 2×CH_3), 0.84 (s, 3H, CH_3).

*4.2.3. General procedure for preparation of compound **6a-6k**.*

Compound **4** (1 mmol) added to dry CH_2Cl_2 (15 mL) was stirred at 0 ^{o}C and oxalyl chloride (2.0 mmol) was dripped into the mixture and stirred at the same temperature for 12 h. After the reaction, the solvent and excess oxalyl chloride was evaporated under the reduced pressure, then add $CHCl_3$. Compounds **2** (1 mmol) and triethylamine (1.5 mmol) were added to the mixture and reflux at 65 ^{o}C for 5 h. After the reaction, the solvent was evaporated under reduced pressure, and the crude product was purified by chromatography on silica gel eluted with petroleum CH_2Cl_2/CH_3OH (V: V = 60:1) to offer the target compounds **6a**-**6k** in good yields.

*18β-3-O-Acetyl-11-oxo-olean-12-en-30-benzothiazolyl-amide (**6a**).* This was obtained as a light yellow solid (495 mg, 77%).^{1}H NMR (300 MHz, $CDCl_3$) δ 9.29 (s, 1H, NH), 7.80 (d, *J* = 7.8 Hz, 1H), 7.73 (d, *J* = 8.0 Hz, 1H), 7.42 (t, *J* = 7.6 Hz, 1H), 7.31 (d, *J* = 7.8 Hz, 1H), 5.81 (s, 1H), 4.60 – 4.49 (m, 1H), 2.89 – 2.75 (m, 1H), 2.38 (s, 1H), 2.30 – 2.21 (m, 1H), 2.05 (s, 3H, CH_3), 2.04 – 1.80 (m, 4H), 1.78 – 1.55 (m, 6H), 1.54 – 1.41 (m, 4H), 1.39 (s, 3H, CH_3), 1.29 (s, 3H, CH_3), 1.24 (d, *J* = 9.1 Hz, 2H), 1.15 (d, *J* = 8.6 Hz, 6H, 2×CH_3), 1.10 – 0.99 (m, 2H), 0.88 (s, 6H, 2×CH_3), 0.83 (s, 3H, CH_3). ^{13}C NMR (75 MHz, $CDCl_3$) δ 199.34, 173.91, 170.50, 167.72, 157.55, 147.81, 131.75, 128.40, 125.70, 123.39, 120.85, 120.40, 80.14, 61.25, 54.56, 47.28, 44.93, 43.90, 42.70, 40.52, 38.35, 37.57, 36.93, 36.49, 32.23, 31.49, 30.91, 29.19, 28.28, 27.88, 27.57, 25.91, 23.08, 22.93, 20.80, 18.21, 16.90, 16.19, 15.90. HR-MS (m/z) (ESI): calcd for $C_{39}H_{52}N_2O_4S$ [M-H$^+$]: 643.3570; found: 643.3554.

*18β-3-O-Acetyl-11-oxo-olean-12-en-30-(4'-methylbenzothiazolyl)amide (**6b**).* This was obtained as a light yellow solid (475 mg, 75%). ^{1}H NMR (300 MHz, $CDCl_3$) δ 9.33 (s, 1H, NH), 7.57 (d, *J* = 6.9 Hz, 1H), 7.20 – 7.12 (m, 2H), 5.85 (s, 1H), 4.58 – 4.50 (m, 1H), 2.83 (d, *J* = 13.5 Hz, 1H),

2.57 (s, 3H, CH_3), 2.38 (s, 1H), 2.25 (d, *J* = 11.9 Hz, 1H), 2.06 (s, 3H, CH_3), 2.05 – 1.79 (m, 4H), 1.78 – 1.51 (m, 6H), 1.46 (d, *J* = 14.5 Hz, 4H), 1.39 (s, 3H, CH_3), 1.31 (s, 3H, CH_3), 1.26 (s, 2H), 1.15 (d, *J* = 11.2 Hz, 6H, 2×CH_3), 1.10 – 1.02 (m, 2H), 0.89 (s, 6H, 2×CH_3), 0.83 (s, 3H, CH_3). ^{13}C NMR (75 MHz, $CDCl_3$) δ 199.48, 173.87, 170.51, 168.11, 156.38, 146.93, 131.37, 130.03, 128.22, 126.20, 123.19, 118.19, 80.14, 61.28, 54.56, 47.44, 44.94, 43.92, 42.71, 40.67, 38.37, 37.57, 36.90, 36.46, 32.24, 31.53, 30.90, 29.19, 28.14, 27.83, 27.57, 25.93, 23.06, 22.94, 20.80, 18.20, 17.70, 16.89, 16.20, 15.85. HR-MS (m/z) (ESI): calcd for $C_{40}H_{54}N_2O_4S$ [M+Na^+]: 657.3762; found: 657.3777.

*18β-3-O-Acetyl-11-oxo-olean-12-en-30-(6'-methylbenzothiazolyl)amide (**6c**)*. This was obtained as a light yellow solid (506 mg, 77%). ^{1}H NMR (300 MHz, $CDCl_3$) δ 9.26 (s, 1H, NH), 7.60 (d, *J* = 8.4 Hz, 2H), 7.23 (d, *J* = 9.0 Hz, 1H), 5.80 (s, 1H), 4.57 – 4.50 (m, 1H), 2.82 (d, *J* = 13.7 Hz, 1H), 2.46 (s, 3H, CH_3), 2.37 (s, 1H), 2.26 (d, *J* = 11.2 Hz, 1H), 2.05 (s, 3H, CH_3), 2.04 – 1.84 (m, 4H), 1.81 – 1.58 (m, 6H), 1.53 – 1.41 (m, 4H), 1.39 (s, 3H, CH_3), 1.28 (s, 3H, CH_3), 1.26 (s, 2H), 1.14 (d, *J* = 10.0 Hz, 6H, 2×CH_3), 1.05 (d, *J* = 13.4 Hz, 2H), 0.88 (s, 6H, 2×CH_3), 0.82 (s, 3H, CH_3). ^{13}C NMR (75 MHz, $CDCl_3$) δ 199.30, 173.82, 170.48, 167.72, 156.78, 145.69, 133.37, 131.85, 128.39, 127.18, 120.61, 119.91, 80.14, 61.25, 54.56, 47.24, 44.91, 43.86, 42.70, 40.54, 38.34, 37.57, 36.94, 36.48, 32.23, 31.48, 30.90, 29.19, 28.31, 27.87, 27.57, 25.91, 23.08, 22.93, 20.95, 20.79, 18.20, 16.90, 16.19, 15.89. HR-MS (m/z) (ESI): calcd for $C_{40}H_{54}N_2O_4S$ [M-H^+]: 657.3762; found: 657.3723.

*18β-3-O-Acetyl-11-oxo-olean-12-en-30-(4'-methoxylbenzothiazolyl)amide (**6d**)*. This was obtained as a light yellow solid (471 mg, 70%). ^{1}H NMR (500 MHz, $CDCl_3$) δ 8.51 (d, *J* = 8.5 Hz, 1H, NH), 8.20 (s, 1H), 7.22 – 7.19 (m, 1H), 7.12 (d, *J* = 2.0 Hz, 1H), 5.78 (s, 1H), 4.59 – 4.54 (m, 1H), 4.07 (s, 3H, OCH_3), 2.90 – 2.82 (m, 1H), 2.43 (s, 1H), 2.31 – 2.25 (m, 1H), 2.22 – 2.10 (m, 2H), 2.09 (s, 3H, CH_3), 2.09 – 1.90 (m, 2H), 1.90 – 1.66 (m, 6H), 1.65 – 1.46 (m, 4H), 1.46 (s, 3H, CH_3), 1.30 (s, 3H, CH_3), 1.29 (s, 2H), 1.19 (d, *J* = 15.7 Hz, 6H, 2×CH_3), 1.15 – 1.08 (m, 2H), 0.93 (s, 6H, 2×CH_3), 0.86 (s, 3H, CH_3). ^{13}C NMR (126 MHz, $CDCl_3$) δ 199.87, 174.09, 170.93, 168.99, 148.93, 129.53, 128.53, 124.61, 120.64, 117.24, 112.50, 110.91, 80.55, 61.88, 56.29, 55.08, 48.24, 45.34, 43.22, 42.17, 38.93, 38.06, 37.40, 37.03, 32.70, 31.98, 31.43, 29.65, 29.40, 28.44, 28.04, 26.45, 26.36, 23.54, 23.40, 21.24, 18.71, 17.36, 16.65, 16.40. HR-MS (m/z) (ESI): calcd for $C_{40}H_{54}N_2O_5S$ [M-H^+]: 673.3675; found: 673.3660.

18β-3-O-Acetyl-11-oxo-olean-12-en-30-(6'-methoxylbenzothiazolyl)amide ***(6e)***. This was obtained as a light yellow solid (485 mg, 72%). ^{1}H NMR (500 MHz, $CDCl_3$) δ 9.25 (s, 1H, NH), 7.65 (d, *J* = 8.8 Hz, 1H), 7.31 (s, 1H), 7.07 – 7.04 (m, 1H), 5.84 (s, 1H), 4.59 – 4.54 (m, 1H), 3.90 (s, 3H, OCH_3), 2.88 – 2.83 (m, 1H), 2.41 (s, 1H), 2.29 (d, *J* = 13.3 Hz, 1H), 2.09 (s, 3H, CH_3), 2.06 – 1.84 (m, 4H), 1.73 – 1.58 (m, 6H), 1.52 – 1.45 (m, 4H), 1.43 (s, 3H, CH_3), 1.31 (s, 3H, CH_3), 1.30 (s, 2H), 1.20 (s, 3H, CH_3), 1.16 (s, 3H, CH_3), 1.12 – 1.07 (m, 2H), 0.92 (s, 6H, 2× CH_3), 0.86 (s, 3H, CH_3). ^{13}C NMR (125 MHz, $CDCl_3$) δ 199.78, 174.19, 170.95, 168.22, 156.81, 156.06, 142.50, 133.44, 128.86, 121.43, 115.18, 104.24, 80.63, 61.73, 55.82, 55.05, 47.76, 45.40, 44.30, 43.19, 41.04, 38.83, 38.05, 37.41, 36.97, 32.72, 31.96, 31.37, 29.66, 28.79, 28.35, 28.05, 26.41, 23.55, 23.40, 21.25, 18.69, 17.38, 16.66, 16.36. HR-MS (m/z) (ESI): calcd for $C_{40}H_{54}N_2O_5S$ [M-H$^+$]: 673.3675; found: 673.3677.

18β-3-O-Acetyl-11-oxo-olean-12-en-30-(4'-fluorobenzothiazolyl)amide ***(6f)***. This was obtained as a light yellow solid (496 mg, 75%). ^{1}H NMR (500 MHz, $CDCl_3$) δ 9.46 (s, 1H, NH), 7.51 (d, *J* = 7.8 Hz, 1H), 7.23 – 7.17 (m, 1H), 7.13 – 7.08 (m, 1H), 5.87 (s, 1H), 4.57 – 4.50 (m, 1H), 2.82 (d, *J* = 13.7 Hz, 1H), 2.38 (s, 1H), 2.27 (d, *J* = 10.3 Hz, 1H), 2.05 (s, 3H, CH_3), 2.04 – 1.75 (m, 4H), 1.72 – 1.56 (m, 6H), 1.49 – 1.41 (m, 4H), 1.39 (s, 3H, CH_3), 1.31 (s, 3H, CH_3), 1.29 (s, 2H), 1.17 (s, 3H, CH_3), 1.13 (s, 3H, CH_3), 1.06 (d, *J* = 13.4 Hz, 2H), 0.89 (d, *J* = 3.0 Hz, 6H, 2×CH_3), 0.84 (s, 3H, CH_3). ^{13}C NMR (125 MHz, $CDCl_3$) δ 199.91, 174.53, 170.95, 168.36, 158.18, 155.70, 134.99, 128.77, 124.36, 124.31, 116.95, 111.94, 111.80, 80.62, 61.73, 55.04, 47.74, 45.44, 44.43, 43.17, 40.98, 38.86, 38.06, 37.36, 36.95, 32.74, 32.00, 31.48, 29.67, 28.55, 28.24, 28.05, 26.43, 23.56, 23.41, 21.26, 18.68, 17.39, 16.68, 16.34. HR-MS (m/z) (ESI): calcd for $C_{39}H_{51}FN_2O_4S$ [M-H$^+$]: 661.3476; found: 661.3458.

18β-3-O-Acetyl-11-oxo-olean-12-en-30-(6'-fluorobenzothiazolyl)amide ***(6g)***. This was obtained as a light yellow solid (483 mg, 73%). ^{1}H NMR (500 MHz, $CDCl_3$) δ 9.37 (s, 1H, NH), 7.66-7.61 (m, 1H), 7.49 – 7.45 (m, 1H), 7.16 – 7.11 (m, 1H), 5.82 (s, 1H), 4.56 – 4.51 (m, 1H), 2.82 (d, *J* = 13.6 Hz, 1H), 2.38 (s, 1H), 2.23 (d, *J* = 13.7 Hz, 1H), 2.05 (s, 3H, CH_3), 2.02 – 1.80 (m, 4H), 1.72 – 1.55 (m, 6H), 1.48 – 1.41 (m, 4H), 1.39 (s, 3H, CH_3), 1.29 (s, 3H, CH_3), 1.26 (s, 2H), 1.15 (d, *J* = 13.0 Hz, 6H, 2×CH_3), 1.10 – 1.04 (m, 2H), 0.89 (d, *J* = 2.5 Hz, 6H, 2×CH_3), 0.84 (s, 3H, CH_3). ^{13}C NMR (125 MHz, $CDCl_3$) δ 199.90, 174.49, 170.97, 168.27, 160.54, 144.77, 128.84, 121.71, 121.64, 114.60, 114.41, 107.66, 107.45, 80.62, 61.75, 55.05, 47.91, 45.45, 44.38,

43.20, 41.03, 38.84, 38.05, 37.38, 36.98, 32.72, 31.99, 31.35, 29.66, 28.68, 28.36, 28.04, 26.41, 23.55, 23.41, 21.26, 18.69, 17.38, 16.66, 16.36. HR-MS (m/z) (ESI): calcd for $C_{39}H_{51}FN_2O_4S$ [M-H^+]: 661.3476; found: 661.3460.

*18β-3-O-Acetyl-11-oxo-olean-12-en-30-(4'-chlorobenzothiazolyl)amide (**6h**).* This was obtained as a light yellow solid (514 mg, 76%). ^{1}H NMR (500 MHz, $CDCl_3$) δ 8.58 (d, *J* = 8.8 Hz, 1H, NH), 8.07 (s, 1H), 7.66 (d, *J* = 2.2 Hz, 1H), 7.52 – 7.49 (m, 1H), 5.76 (s, 1H), 4.59 – 4.54 (m, 1H), 2.87 – 2.81 (m, 1H), 2.41 (s, 1H), 2.28 (d, *J* = 13.2 Hz, 1H), 2.09 (s, 3H, CH_3), 2.06 – 1.85 (m, 4H), 1.75 – 1.57 (m, 6H), 1.55 – 1.46 (m, 4H), 1.44 (s, 3H, CH_3), 1.33 (s, 3H, CH_3), 1.30 (s, 2H), 1.18 (d, *J* = 17.6 Hz, 6H, 2×CH_3), 1.14 – 1.07 (m, 2H), 0.92 (s, 6H, 2×CH_3), 0.87 (s, 3H, CH_3). ^{13}C NMR (125 MHz, $CDCl_3$) δ 199.67, 174.36, 170.94, 168.21, 136.42, 131.10, 130.61, 128.81, 124.05, 122.45, 118.65, 109.96, 80.58, 61.77, 55.05, 47.91, 45.37, 43.23, 41.71, 38.85, 38.05, 37.41, 36.98, 32.74, 32.01, 31.67, 29.66, 29.40, 28.37, 28.05, 26.44, 26.40, 23.56, 23.39, 21.25, 18.70, 17.39, 16.66, 16.37. HR-MS (m/z) (ESI): calcd for $C_{39}H_{51}ClN_2O_4S$ [M-H^+]: 677.3180; found: 678.3177.

*18β-3-O-Acetyl-11-oxo-olean-12-en-30-(6'-chlorobenzothiazolyl)amide (**6i**).* This was obtained as a light yellow solid (541 mg, 80%). ^{1}H NMR (500 MHz, $CDCl_3$) δ 9.56 (s, 1H, NH), 7.77 (d, *J* = 1.9 Hz, 1H), 7.61 (d, *J* = 8.6 Hz, 1H), 7.41 – 7.38 (m, 1H), 5.88 (s, 1H), 4.59 – 4.55 (m, 1H), 2.85 (d, *J* = 13.7 Hz, 1H), 2.42 (s, 1H), 2.28 – 2.24 (m, 1H), 2.09 (s, 3H, CH_3), 1.92 – 1.82 (m, 4H), 1.76 – 1.59 (m, 6H), 1.50 (d, *J* = 19.3 Hz, 4H), 1.43 (s, 3H, CH_3), 1.34 (s, 3H, CH_3), 1.33 (s, 2H), 1.19 (d, *J* = 11.4 Hz, 6H, 2×CH_3), 1.14 – 1.09 (m, 2H), 0.93 (d, *J* = 3.9 Hz, 6H, 2×CH_3), 0.88 (s, 3H, CH_3). ^{13}C NMR (125 MHz, $CDCl_3$) δ 200.04, 174.63, 170.98, 168.43, 158.35, 146.95, 133.49, 129.28, 128.79, 126.83, 121.58, 120.88, 80.62, 61.76, 55.05, 48.02, 45.49, 44.45, 43.22, 41.03, 38.85, 38.06, 37.37, 36.98, 32.72, 32.02, 31.36, 29.67, 28.57, 28.39, 28.05, 26.42, 23.55, 23.41, 21.27, 18.70, 17.39, 16.67, 16.35. HR-MS (m/z) (ESI): calcd for $C_{39}H_{51}ClN_2O_4S$ [M-H^+]: 677.3180; found: 677.3182.

*18β-3-O-Acetyl-11-oxo-olean-12-en-30-(4'-bromobenzothiazolyl)amide (**6j**).* This was obtained as a light yellow solid (511 mg, 71%). ^{1}H NMR (500 MHz, $CDCl_3$) δ 9.37 (s, 1H, NH), 7.72 (d, *J* = 7.9 Hz, 1H), 7.60 (d, *J* = 7.8 Hz, 1H), 7.14 (t, *J* = 7.9 Hz, 1H), 5.82 (s, 1H), 4.57 – 4.50 (m, 1H), 2.82 (d, *J* = 13.7 Hz, 1H), 2.38 (s, 1H), 2.30 – 2.24 (m, 1H), 2.05 (s, 3H, CH_3), 2.00 – 1.76 (m, 4H), 1.73 – 1.57 (m, 6H), 1.51 – 1.41 (m, 4H), 1.39 (s, 3H, CH_3), 1.29 (s, 3H, CH_3), 1.26 (s, 2H),

1.17 (s, 3H, CH_3), 1.13 (s, 3H, CH_3), 1.06 (d, *J* = 11.0 Hz, 2H), 0.89 (s, 6H, 2×CH_3), 0.82 (s, 3H, CH_3). ^{13}C NMR (125 MHz, $CDCl_3$) δ 199.78, 174.64, 170.95, 168.19, 158.50, 146.68, 133.05, 129.51, 128.88, 124.72, 120.56, 114.37, 80.62, 61.75, 55.06, 47.62, 45.40, 44.46, 43.18, 40.92, 38.85, 38.06, 37.43, 36.96, 32.73, 31.97, 31.39, 29.66, 28.58, 28.35, 28.05, 26.40, 23.56, 23.43, 21.26, 18.69, 17.38, 16.67, 16.36. HR-MS (m/z) (ESI): calcd for $C_{39}H_{52}BrN_2O_4S$ [M-H$^+$]: 721.2675; found: 721.2676.

*18β-3-O-Acetyl-11-oxo-olean-12-en-30-(6'-bromobenzothiazolyl)amide (**6k**)*. This was obtained as a light yellow solid (526 mg, 73%). ^{1}H NMR (300 MHz, $CDCl_3$) δ 9.64 (s, 1H, NH), 7.86 (s, 1H), 7.48 (s, 2H), 5.88 (s, 1H), 4.56 – 4.50 (m, 1H), 2.81 (d, *J* = 13.6 Hz, 1H), 2.38 (s, 1H), 2.20 (d, *J* = 13.3 Hz, 1H), 2.05 (s, 3H, CH_3), 2.04 – 1.79 (m, 4H), 1.78 – 1.52 (m, 6H), 1.51 – 1.42 (m, 4H), 1.38 (s, 3H, CH_3), 1.31 (s, 3H, CH_3), 1.26 (s, 2H), 1.15 (d, *J* = 4.9 Hz, 6H, 2×CH_3), 1.11 – 1.04 (m, 2H), 0.88 (d, *J* = 3.2 Hz, 6H, 2×CH_3), 0.85 (s, 3H, CH_3). ^{13}C NMR (75 MHz, $CDCl_3$) δ 199.69, 174.22, 170.51, 168.13, 157.80, 146.84, 133.45, 129.01, 128.24, 123.25, 121.45, 116.14, 80.13, 61.26, 54.54, 47.65, 45.03, 43.99, 42.72, 40.53, 38.37, 37.56, 36.86, 36.47, 32.22, 31.54, 30.89, 29.19, 27.98, 27.93, 27.56, 25.94, 23.05, 22.92, 20.80, 18.21, 16.89, 16.19, 15.85. HR-MS (m/z) (ESI): calcd for $C_{39}H_{52}BrN_2O_4S$ [M-H$^+$]: 721.2675; found: 721.2687.

*4.2.4. General procedure for preparation of the target compounds **7a-7k**.*

1 M NaOH aq. (180 mL, 0.18 mmol, 1.5 equiv) was added dropwise to a solution of compound **6** (0.12 mmol, 1.0 equiv) in methanol (2 mL) and tetrahydrofuran (1 mL) at room temperature. The resulting solution was stirred at 40 ^{o}C for 5 h. Progress of the reaction was monitored by TLC. After completion of the reaction, the solvent was removed under reduced pressure. The resulting mixture was diluted with water (100 mL) and extracted with dichloromethane (50 mL × 2). The combined organic layers were washed with brine (50 mL) and dried over anhydrous sodium sulfate. After evaporation of the solvent, the crude residue was purified by column chromatography on silica gel eluted with petroleum CH_2Cl_2/CH_3OH (V: V = 50:1) to give the compound **7a-7k** in good yields.

*18β-11-Oxo-olean-12-en-30-benzothiazolyl-amide (**7a**)*. This was obtained as a light yellow solid (51 mg, 71%). ^{1}H NMR (500 MHz, $CDCl_3$) δ 9.94 (s, 1H, NH), 7.80 (d, *J* = 7.9 Hz, 1H), 7.72 (d, *J* = 8.1 Hz, 1H), 7.42 (t, *J* = 7.7 Hz, 1H), 7.31 – 7.27 (m, 1H), 5.75 (s, 1H), 3.25 – 3.20 (m, 1H), 2.78 (d, *J* = 13.6 Hz, 1H), 2.34 (s, 1H), 2.17 (d, *J* = 12.8 Hz, 1H), 2.11 – 2.02 (m, 4H), 1.90 –

1.80 (m, 2H), 1.71 – 1.60 (m, 4H), 1.52 – 1.43 (m, 4H), 1.41 (s, 3H, CH_3), 1.29 (s, 3H, CH_3), 1.26 (s, 2H), 1.13 (d, *J* = 8.9 Hz, 6H, 2×CH_3), 1.06 (d, *J* = 13.9 Hz, 1H), 1.03 (s, 3H, CH_3), 0.92 – 0.88 (m, 1H), 0.83 (d, *J* = 6.5 Hz, 6H, 2×CH_3). ^{13}C NMR (126 MHz, $CDCl_3$) δ 199.52, 174.63, 167.98, 158.53, 148.23, 132.10, 128.74, 126.15, 123.79, 121.30, 120.81, 79.19, 61.89, 55.15, 48.12, 45.44, 44.36, 43.17, 41.09, 39.58, 39.22, 37.31, 37.08, 32.83, 32.03, 31.11, 28.71, 28.26, 28.17, 27.26, 26.47, 26.40, 23.51, 18.66, 17.55, 16.31, 15.59. HR-MS (m/z) (ESI): calcd for $C_{37}H_{50}N_2O_3S$ [M-H^+]: 601.3464; found: 601.3461.

*18β-11-Oxo-olean-12-en-30-(4'-methylbenzothiazolyl)amide (**7b**).* This was obtained as a light yellow solid (51 mg, 69%). ^{1}H NMR (300 MHz, $CDCl_3$) δ 10.18 (s, 1H, NH), 7.67 – 7.58 (m, 1H), 7.20 (q, *J* = 7.6 Hz, 2H), 5.74 (s, 1H), 3.25 – 3.13 (m, 1H), 2.79 (s, 1H), 2.61 (s, 3H, CH_3), 2.57 – 2.36 (m, 1H), 2.32 (s, 1H), 2.13 (d, *J* = 12.9 Hz, 2H), 2.03 – 1.83 (m, 4H), 1.72 – 1.58 (m, 4H), 1.50 (d, *J* = 9.7 Hz, 4H), 1.43 (s, 3H, CH_3), 1.30 (s, 3H, CH_3), 1.23 (d, *J* = 15.9 Hz, 2H), 1.14 (d, *J* = 6.8 Hz, 6H, 2×CH_3), 1.10 – 1.06 (m, 1H), 1.03 (s, 3H, CH_3), 1.00 – 0.86 (m, 1H), 0.83 (d, *J* = 5.0 Hz, 6H, 2×CH_3). ^{13}C NMR (75 MHz, $CDCl_3$) δ 199.35, 174.47, 168.05, 157.56, 147.35, 131.73, 130.37, 128.52, 126.76, 123.68, 118.75, 79.41, 61.90, 55.24, 48.40, 45.46, 44.34, 43.14, 41.30, 39.85, 39.25, 37.22, 37.04, 32.83, 32.10, 30.98, 28.67, 28.18, 28.11, 27.27, 26.51, 26.35, 23.57, 18.63, 18.11, 17.54, 16.30, 15.49. HR-MS (m/z) (ESI): calcd for $C_{38}H_{52}N_2O_3S$ [M-H^+]: 615.3621; found: 615.3628.

*18β-11-Oxo-olean-12-en-30-(6'-methylbenzothiazolyl)amide (**7c**).* This was obtained as a light yellow solid (50 mg, 68%). ^{1}H NMR (300 MHz, $CDCl_3$) δ 9.67 (s, 1H, NH), 7.60 (s, 2H), 7.23 (d, *J* = 7.0 Hz, 1H), 5.76 (s, 1H), 3.27 – 3.18 (m, 1H), 2.79 (d, *J* = 13.6 Hz, 1H), 2.47 (s, 3H, CH_3), 2.34 (s, 1H), 2.20 (d, *J* = 11.3 Hz, 1H), 2.05 (d, *J* = 14.0 Hz, 2H), 1.93 – 1.74 (m, 4H), 1.69 – 1.58 (m, 4H), 1.53 – 1.43 (m, 4H), 1.41 (s, 3H, CH_3), 1.27 (d, *J* = 6.7 Hz, 6H, 2×CH_3), 1.14 (s, 3H, CH_3), 1.12 – 1.09 (m, 2H), 1.02 (s, 3H, CH_3), 0.97 – 0.86 (m, 2H), 0.82 (s, 6H, 2×CH_3). ^{13}C NMR (75 MHz, DMSO) δ 199.18, 173.97, 167.57, 157.14, 145.72, 133.40, 128.36, 127.23, 123.33, 120.68, 119.94, 78.63, 61.43, 54.66, 47.52, 44.98, 43.90, 42.73, 40.66, 39.02, 38.78, 36.90, 36.65, 32.38, 31.58, 30.77, 29.24, 28.36, 27.84, 27.71, 26.84, 25.97, 23.07, 21.00, 18.23, 17.09, 15.89, 15.14. HR-MS (m/z) (ESI): calcd for $C_{38}H_{52}N_2O_3S$ [M-H^+]: 615.3621; found: 615.3600.

*18β-11-Oxo-olean-12-en-30-(4'-methoxylbenzothiazolyl)amide (**7d**).* This was obtained as a light yellow solid (56 mg, 74%). ^{1}H NMR (500 MHz, $CDCl_3$) δ 8.55 – 8.49 (m, 1H, NH), 8.22 (s,

1H), 7.40 – 7.33 (m, 1H), 7.15 – 7.06 (m, 1H), 5.76 (d, *J* = 2.7 Hz, 1H), 4.08 (d, *J* = 5.1 Hz, 3H, OCH_3), 3.27 – 3.20 (m, 1H), 2.82 (d, *J* = 13.5 Hz, 1H), 2.38 (s, 1H), 2.26 (d, *J* = 13.4 Hz, 1H), 2.22 – 2.07 (m, 2H), 2.06 – 1.76 (m, 4H), 1.69 – 1.60 (m, 6H), 1.47– 1.44 (m, 2H), 1.43 (s, 3H, CH_3), 1.26 (s, 3H, CH_3), 1.26 – 1.25 (m, 2H), 1.14 (d, *J* = 1.8 Hz, 6H, 2×CH_3), 1.07 (d, *J* = 13.8 Hz, 1H), 1.02 (s, 3H, CH_3), 0.93 – 0.85 (m, 1H), 0.82 (d, *J* = 6.5 Hz, 6H, 2×CH_3). ^{13}C NMR (126 MHz, $CDCl_3$) δ 200.08, 174.13, 168.99, 148.61, 137.72, 128.62, 119.87, 119.79, 116.76, 116.61, 104.62, 78.73, 61.98, 56.35, 55.02, 48.19, 45.33, 44.35, 44.29, 43.23, 39.29, 39.16, 37.43, 37.19, 32.78, 32.00, 29.66, 29.47, 28.45, 28.10, 27.30, 26.49, 26.38, 23.47, 18.72, 17.49, 16.37, 15.55. HR-MS (m/z) (ESI): calcd for $C_{38}H_{52}N_2O_4S$ [M-H^+]: 633.3726; found: 633.3766.

*18β-11-Oxo-olean-12-en-30-(6'-methoxylbenzothiazolyl)amide (**7e**).* This was obtained as a light yellow solid (53 mg, 70%). ^{1}H NMR (300 MHz, $CDCl_3$) δ 9.75 (s, 1H, NH), 7.61 (d, *J* = 8.9 Hz, 1H), 7.27 (s, 1H), 7.05 – 6.99 (m, 1H), 5.76 (s, 1H), 3.87 (s, 3H, OCH_3), 3.21 (d, *J* = 8.7 Hz, 1H), 2.78 (d, *J* = 13.4 Hz, 1H), 2.34 (s, 1H), 2.18 (d, *J* = 12.5 Hz, 1H), 2.09 –1.99 (m, 4H), 1.90 – 1.78 (m, 2H), 1.72 – 1.59 (m, 4H), 1.46 (d, *J* = 10.7 Hz, 4H), 1.41 (s, 3H, CH_3), 1.28 (s, 3H, CH_3), 1.26 (s, 2H), 1.13 (d, *J* = 5.0 Hz, 6H, 2×CH_3), 1.02 (s, 3H, CH_3), 0.99 – 0.86 (m, 2H), 0.82 (s, 6H, 2×CH_3). ^{13}C NMR (75 MHz, $CDCl_3$) δ 199.17, 173.93, 167.61, 156.33, 142.01, 132.89, 128.31, 126.48, 120.95, 114.74, 103.80, 78.68, 61.44, 55.40, 54.68, 47.60, 44.99, 43.85, 42.73, 40.65, 39.08, 38.77, 36.89, 36.64, 32.38, 31.58, 30.71, 29.23, 28.35, 27.84, 27.72, 26.82, 25.96, 23.07, 18.22, 17.09, 15.88, 15.15. HR-MS (m/z) (ESI): calcd for $C_{38}H_{52}N_2O_4S$ [M-H^+]: 631.3570; found: 631.3544.

*18β-11-Oxo-olean-12-en-30-(4'-fluorobenzothiazolyl)amide (**7f**).* This was obtained as a light yellow solid (51 mg, 69%). ^{1}H NMR (500 MHz, $CDCl_3$) δ 9.73 (s, 1H, NH), 7.55 (d, *J* = 7.7 Hz, 1H), 7.26 – 7.21 (m, 1H), 7.15 – 7.10 (m, 1H), 5.78 (s, 1H), 3.25 – 3.21 (m, 1H), 2.81 – 2.77 (m, 1H), 2.34 (s, 1H), 2.23 – 2.19 (m, 1H), 2.11 – 1.99 (m, 4H), 1.88 – 1.82 (m, 2H), 1.68 – 1.61 (m, 4H), 1.50 – 1.43 (m, 4H), 1.41 (s, 3H, CH_3), 1.29 (s, 3H, CH_3), 1.26 (s, 2H), 1.13 (d, *J* = 8.8 Hz, 6H, 2×CH_3), 1.09 – 1.05 (m, 1H), 1.02 (s, 3H, CH_3), 0.97 – 0.91 (m, 1H), 0.83 (d, *J* = 1.6 Hz, 6H, 2×CH_3). ^{13}C NMR (125 MHz, $CDCl_3$) δ 199.64, 174.58, 167.92, 158.46, 137.04, 128.81, 124.44, 124.39, 117.02, 116.95, 111.98, 111.84, 79.06, 61.86, 55.09, 47.93, 45.42, 44.39, 43.16, 41.05, 39.41, 39.17, 37.32, 37.08, 32.83, 32.03, 31.26, 29.67, 28.66, 28.24, 28.12, 27.28, 26.45, 23.51,

18.66, 17.53, 16.30, 15.52. HR-MS (m/z) (ESI): calcd for $C_{37}H_{49}FN_2O_4S$ [M-H^+]: 619.3370; found: 619.3334.

*18β-11-Oxo-olean-12-en-30-(6'-fluorobenzothiazolyl)amide (**7g**).* This was obtained as a light yellow solid (57 mg, 77%). ^{1}H NMR (300 MHz, $CDCl_3$) δ 9.87 (s, 1H, NH), 7.68 – 7.61 (m, 1H), 7.51-7.45 (m, 1H), 7.19-7.11 (m, 1H), 5.75 (s, 1H), 3.25 – 3.18 (m, 1H), 2.78 (d, *J* = 13.5 Hz, 1H), 2.33 (s, 1H), 2.15 (d, *J* = 13.3 Hz, 1H), 2.05 (d, *J* = 9.8 Hz, 2H), 1.99 – 1.79 (m, 4H), 1.70 – 1.60 (m, 4H), 1.54 – 1.45 (m, 4H), 1.41 (s, 3H, CH_3), 1.29 (s, 3H, CH_3), 1.26 (s, 2H), 1.13 (d, *J* = 3.5 Hz, 6H, 2×CH_3), 1.05 (s, 1H), 1.02 (s, 3H, CH_3), 0.90 (d, *J* = 11.0 Hz, 1H), 0.83 (s, 6H, 2×CH_3). ^{13}C NMR (75 MHz, $CDCl_3$) δ 199.15, 174.18, 167.59, 157.51, 144.32, 128.28, 121.30, 121.18, 114.23, 113.91, 107.31, 106.96, 78.77, 61.46, 54.72, 47.74, 45.02, 43.91, 42.73, 40.65, 39.16, 38.78, 36.84, 36.64, 32.38, 31.61, 30.67, 28.28, 27.83, 27.72, 26.82, 26.02, 25.94, 23.08, 18.22, 17.09, 15.87, 15.11. HR-MS (m/z) (ESI): calcd for $C_{37}H_{49}FN_2O_4S$ [M-H^+]: 619.3370; found: 619.3344.

*18β-11-Oxo-olean-12-en-30-(4'-chlorobenzothiazolyl)amide (**7h**).* This was obtained as a light yellow solid (54 mg, 71%). ^{1}H NMR (300 MHz, $CDCl_3$) δ 9.88 (s, 1H, NH), 7.92 (d, *J* = 1.4 Hz, 1H), 7.56 (d, *J* = 8.6 Hz, 1H), 7.55 – -7.49 (m, 1H), 5.77 (s, 1H), 3.25 – 3.19 (m, 1H), 2.78 (d, *J* = 13.6 Hz, 1H), 2.34 (s, 1H), 2.15 (d, *J* = 13.6 Hz, 1H), 2.09 – 1.98 (m, 4H), 1.88 (d, *J* = 13.8 Hz, 2H), 1.69 – 1.60 (m, 4H), 1.53 – 1.46 (m, 4H), 1.41 (s, 3H, CH_3), 1.29 (s, 3H, CH_3), 1.26 (s, 2H), 1.14 (d, *J* = 3.1 Hz, 6H, 2×CH_3), 1.03 (s, 3H, CH_3), 0.94 – 0.88 (m, 2H), 0.83 (s, 6H, 2×CH_3). ^{13}C NMR (75 MHz, $CDCl_3$) δ 200.15, 176.34, 168.42, 156.66, 144.45, 132.04, 128.79, 128.51,127.31, 126.72, 122.12, 78.75, 61.82, 60.28, 54.97, 48.38, 43.82, 43.21, 41.81, 41.10, 39.12, 37.72, 37.10, 32.78, 31.12, 28.54, 28.29, 28.09, 27.31, 26.49, 26.44, 23.37, 18.68, 17.49, 16.32, 15.55, 14.30. HR-MS (m/z) (ESI): calcd for $C_{37}H_{49}ClN_2O_4S$ [M-H^+]: 635.3074; found: 635.3075.

*18β-11-Oxo-olean-12-en-30-(6'-chlorobenzothiazolyl)amide (**7i**).* This was obtained as a light yellow solid (53 mg, 70%). ^{1}H NMR (500 MHz, $CDCl_3$) δ 9.85 (s, 1H, NH), 7.76 (d, *J* = 2.0 Hz, 1H), 7.61 (d, *J* = 8.6 Hz, 1H), 7.39 – -7.35 (m, 1H), 5.76 (s, 1H), 3.24 – 3.19 (m, 1H), 2.80 – 2.76 (m, 1H), 2.34 (s, 1H), 2.16 (d, *J* = 13.0 Hz, 1H), 2.07 (d, *J* = 8.1 Hz, 2H), 1.92 – 1.76 (m, 4H), 1.68 – 1.61 (m, 4H), 1.54 – 1.45 (m, 4H), 1.41 (s, 3H, CH_3), 1.29 (s, 3H, CH_3), 1.26 (s, 2H), 1.13 (d, *J* = 5.9 Hz, 6H, 2×CH_3), 1.07 (d, *J* = 13.6 Hz, 1H), 1.02 (s, 3H, CH_3), 0.95 – -0.89 (m, 1H),

0.83 (d, *J* = 1.6 Hz, 6H, 2×CH_3). ^{13}C NMR (125 MHz, $CDCl_3$) δ 199.61, 174.67, 168.00, 158.65, 146.93, 133.43, 129.29, 128.74, 126.86, 121.62, 120.92, 79.17, 61.90, 55.15, 48.17, 45.46, 44.39, 43.17, 41.08, 39.56, 39.20, 37.28, 37.09, 32.82, 32.05, 31.13, 29.67, 28.67, 28.27, 28.15, 27.27, 26.46, 23.51, 18.66, 17.53, 16.31, 15.54. HR-MS (m/z) (ESI): calcd for $C_{37}H_{49}ClN_2O_4S$ [M-H$^+$]: 635.3074; found: 635.3057.

*18β-11-Oxo-olean-12-en-30-(4'-bromobenzothiazolyl)amide (**7j**).* This was obtained as a light yellow solid (63 mg, 77%). ^{1}H NMR (500 MHz, $CDCl_3$) δ 10.35 (s, 1H, NH), 7.79 – 7.76 (m, 1H), 7.67 – 7.64 (m, 1H), 7.19 (t, *J* = 7.9 Hz, 1H), 5.77 (s, 1H), 3.29 – 3.21 (m, 1H), 2.82 (d, *J* = 2.7 Hz, 1H), 2.37 (d, *J* = 12.3 Hz, 2H), 2.15 – 2.05 (m, 4H), 1.98 – 1.90 (m, 2H), 1.72 – 1.65 (m, 4H), 1.58 – 1.51 (m, 4H), 1.46 (s, 3H, CH_3), 1.33 (s, 3H, CH_3), 1.31 (s, 2H), 1.19 (d, *J* = 2.4 Hz, 6H, 2×CH_3), 1.13 – 1.09 (m, 1H), 1.07 (s, 3H, CH_3), 1.05 (s, 1H), 0.88 (d, *J* = 14.7 Hz, 6H, 2×CH_3). ^{13}C NMR (125 MHz, $CDCl_3$) δ 199.27, 174.81, 167.77, 158.91, 146.72, 132.93, 129.48, 128.63, 124.64, 120.55, 114.45, 79.50, 61.92, 55.29, 48.27, 45.48, 44.41, 43.14, 41.11, 39.87, 39.30, 37.26, 37.06, 32.86, 32.10, 30.99, 28.60, 28.20, 28.17, 27.24, 26.51, 26.36, 23.59, 18.65, 17.57, 16.33, 15.60. HR-MS (m/z) (ESI): calcd for $C_{37}H_{49}BrN_2O_3S$ [M-H$^+$]: 679.2569; found: 679.2528.

*18β-11-Oxo-olean-12-en-30-(6'-bromobenzothiazolyl)amide (**7k**).* This was obtained as a light yellow solid (60 mg, 73%). ^{1}H NMR (300 MHz, $CDCl_3$) δ 9.88 (s, 1H, NH), 7.91 (d, *J* = 1.4 Hz, 1H), 7.56 (d, *J* = 8.6 Hz, 1H), 7.53 – 7.49 (m, 1H), 5.76 (s, 1H), 3.25 – 3.18 (m, 1H), 2.78 (d, *J* = 13.6 Hz, 1H), 2.33 (s, 1H), 2.15 (d, *J* = 13.6 Hz, 1H), 2.08 – 1.98 (m, 4H), 1.88 (d, *J* = 13.8 Hz, 2H), 1.69 – 1.60 (m, 4H), 1.53 – 1.45 (m, 4H), 1.41 (s, 3H, CH_3), 1.29 (s, 3H, CH_3), 1.26 (s, 2H), 1.13 (d, *J* = 3.1 Hz, 6H, 2×CH_3), 1.02 (s, 3H, CH_3), 0.98 – 0.86 (m, 2H), 0.83 (s, 6H, 2×CH_3). ^{13}C NMR (75 MHz, $CDCl_3$) δ 199.63, 174.69, 168.04, 158.63, 147.27, 134.03, 129.55, 128.71, 123.80, 122.01, 116.69, 79.17, 61.88, 55.13, 48.18, 45.45, 44.39, 43.15, 41.05, 39.56, 39.19, 37.26, 37.06, 32.80, 32.04, 31.11, 28.65, 28.26, 28.14, 27.25, 26.45, 26.36, 23.50, 18.64, 17.51, 16.30, 15.53. HR-MS (m/z) (ESI): calcd for $C_{37}H_{49}BrN_2O_3S$ [M+H$^+$]: 681.2725; found: 681.2738.

*4.2.5. Synthesis of 18β-11-Oxo-olean-12-en-30-oic acidethyl ester(**8**).*

Anhydrous K_2CO_3 (69.1 mg, 0.5 mmol, 1.0 equiv) and EtBr (55.9 mL, 0.75 mmol, 1.5 equiv) were added to a stirred solution of GA 1 (235.3 mg, 0.5 mmol, 1.0 equiv) in acetone (10 mL) at rt. The resulting solution was stirred at 35 ^{o}C for 48 h. Progress of the reaction was monitored by

TLC. After completion of the reaction, the acetone was distilled off. The resulting mixture was diluted with water (15 mL) and extracted with dichloromethane (30 mL×2). The combined organic layers were washed with brine (10 mL) and dried over sodium sulfate. After evaporation of the solvent, the crude residue was purified by column chromatography on silica gel (petroleum ether: ethyl acetate = 3: 1) to give the compound **8** (211 mg, 85%) as the white solid. ^{1}H NMR (300 MHz, $CDCl_3$) δ 5.64 (s, 1H), 4.23 – 4.10 (m, 2H), 3.23 (s, 1H), 2.84 – 2.75 (m, 1H), 2.34 (s, 1H), 2.17 – 1.70 (m, 6H), 1.69 – 1.53 (m, 6H), 1.51 – 1.41 (m, 2H), 1.37 (s, 3H, CH_3), 1.31 (d, *J* = 7.2 Hz, 2H), 1.26 (t, J = 7.0 Hz, 3H, CH_3)., 1.23 – 1.17 (m, 1H), 1.14 (s, 6H, 2×CH_3), 1.13 (s, 3H, CH_3), 1.01 (s, 3H, CH_3), 0.98 – 0.88 (m, 1H), 0.81 (s, 6H, 2×CH_3), 0.70 (d, *J* = 11.5 Hz, 1H).

*4.2.6. Synthesis of 18β-3-O-(β-Carboxypropionyl)-11-oxo-olean-12-en-30-oic acid ethyl ester(**9**)*

Succinic anhydride (50.0 mg, 0.5 mmol, 5 equiv) and DMAP (24.4 mg, 0.2 mmol, 2.0 equiv) were added to a solution of compound **8** (49.8 mg, 0.1 mmol, 1.0 equiv) in dichloromethane (1 mL) at rt. The resulting solution was stirred at rt for 48 h. Progress of the reaction was monitored by TLC. After completion of the reaction, the mixture was acidified with 1 N HCl to pH ~3 and extracted with ethyl acetate (25 mL×3). The combined organic layers were washed with water (10 mL) and brine (10 mL), and dried over sodium sulfate. After evaporation of the solvent, the crude residue was purified by column chromatography on silica gel (dichloromethane: methanol = 20: 1) to get the compound **9** (48 mg, 80%) as the white solid. ^{1}H NMR (300 MHz, $CDCl_3$) δ 5.63 (s, 1H), 4.58 – 4.47 (m, 1H), 4.22 – 4.06 (m, 2H), 2.78 (d, *J* = 13.7 Hz, 1H), 2.70 – 2.58 (m, 4H), 2.34 (s, 1H), 2.13 – 1.89 (m, 4H), 1.88 – 1.57 (m, 6H), 1.55 – 1.38 (m, 3H), 1.35 (s, 3H, CH_3), 1.32 – 1.27 (m, 2H), 1.26 (t, *J* = 6.9 Hz, 3H, CH_3), 1.23 – 1.16 (m, 2H), 1.15 – 1.10 (m, 9H, 3×CH_3), 1.00 (d, *J* = 12.7 Hz, 2H), 0.86 (s, 6H, 2×CH_3), 0.78 (s, 3H, CH_3).

*4.2.7. General procedure for preparation of the target compounds **11a-11k***

Compound **9** (0.1 mmol) added to dry CH_2Cl_2 (15 mL) was stirred at 0 ^{o}C and oxalyl chloride (2.0 mmol) was dripped into the mixture and stirred at the same temperature for 12 h. After the reaction, the solvent and excess oxalyl chloride was evaporated under the reduced pressure, then add $CHCl_3$. Compounds **2** (0.1 mmol) and triethylamine (0.15 mmol) were added to the mixture and reflux at 65 ^{o}C for 5 h. After the reaction, the solvent was evaporated under reduced pressure, and the crude product was purified by chromatography on silica gel eluted with petroleum CH_2Cl_2/CH_3OH (V: V = 60:1) to offer the target compounds **11a-11k** in good yields.

*18β-3-O-(β-(benzothiazolyl)amidepropionyl)-11-oxo-olean-12-en-30-oic acid ethyl ester (**11a**).* This was obtained as a light yellow solid (58 mg, 80%). ^{1}H NMR (500 MHz, $CDCl_3$) δ 10.99 (s, 1H, NH), 7.84 – 7.78 (m, 2H), 7.43 (t, *J* = 7.3 Hz, 1H), 7.31 (t, *J* = 7.6 Hz, 1H), 5.64 (s, 1H), 4.60 – 4.53 (m, 1H), 4.22 – 4.08 (m, 2H), 2.82 – 2.78 (m, 5H), 2.34 (s, 1H), 2.13 – 1.91 (m, 4H), 1.82 – 1.62 (m, 6H), 1.47 – 1.37 (m, 3H), 1.35 (s, 3H, CH_3), 1.34 – 1.28 (m, 2H), 1.26 (t, J = 6.9 Hz, 3H, CH_3), 1.20 – 1.16 (m, 1H), 1.14 (s, 6H, 2×CH_3), 1.11 (s, 3H, CH_3), 1.07 – 0.99 (m, 2H), 0.85 (d, *J* = 9.1 Hz, 6H, 2×CH_3), 0.80 (s, 3H, CH_3), 0.77 (s, 1H). ^{13}C NMR (125 MHz, $CDCl_3$) δ 199.99, 176.36, 172.09, 170.22, 169.35, 158.83, 148.05, 132.06, 128.44, 126.28, 123.94, 121.48, 120.69, 81.58, 61.69, 60.30, 55.05, 48.41, 45.39, 43.83, 43.23, 41.09, 38.76, 38.09, 37.72, 36.94, 32.69, 31.81, 31.26, 31.13, 29.24, 28.54, 28.28, 28.05, 26.49, 26.43, 23.53, 23.31, 18.68, 17.35, 16.65, 16.34, 14.29. HR-MS (m/z) (ESI): calcd for $C_{43}H_{58}N_2O_6S$ [M+H$^+$]: 731.40938; found: 731.40949.

*18β-3-O-(β-(4'-methylbenzothiazolyl)amidepropionyl)-11-oxo-olean-12-en-30-oic acid ethyl ester **(11b).*** This was obtained as a light yellow solid (57 mg, 76%). ^{1}H NMR (300 MHz, $CDCl_3$) δ 9.73 (s, 1H, NH), 7.66 – 7.60 (m, 1H), 7.20 (d, *J* = 7.0 Hz, 2H), 5.65 (s, 1H), 4.60 – 4.53 (m, 1H), 4.21 – 4.10 (m, 2H), 2.80 (s, 5H), 2.61 (s, 3H, CH_3), 2.35 (s, 1H), 2.15 – 1.92 (m, 4H), 1.88 – 1.63 (m, 6H), 1.49 – 1.37 (m, 3H), 1.35 (s, 3H, CH_3), 1.34 – 1.29 (m, 2H), 1.25 (t, J = 6.9 Hz, 3H, CH_3), 1.22 – 1.17 (m, 1H), 1.14 (s, 6H, 2×CH_3), 1.12 (s, 3H, CH_3), 1.05 – 0.98 (m, 2H), 0.86 (d, *J* = 3.5 Hz, 6H, 2×CH_3), 0.80 (s, 3H, CH_3), 0.77 (s, 1H). ^{13}C NMR (75 MHz, $CDCl_3$) δ 200.02, 176.38, 172.10, 169.76, 169.40, 156.64, 147.50, 131.99, 130.72, 128.43, 126.81, 123.83, 118.78, 81.62, 61.68, 60.31, 55.04, 48.41, 45.38, 43.83, 43.22, 41.08, 38.75, 38.10, 37.71, 36.93, 32.68, 31.81, 31.28, 31.12, 29.31, 28.54, 28.29, 28.06, 26.48, 26.42, 23.54, 23.31, 18.67, 18.03, 17.34, 16.67, 16.35, 14.29. HR-MS (m/z) (ESI): calcd for $C_{44}H_{60}N_2O_6S$ [M+H$^+$]: 745.42503; found: 745.42616.

*18β-3-O-(β-(6'-methylbenzothiazolyl)amidepropionyl)-11-oxo-olean-12-en-30-oic acid ethyl ester **(11c).*** This was obtained as a light yellow solid (60 mg, 81%). ^{1}H NMR (300 MHz, $CDCl_3$) δ 11.20 (s, 1H, NH), 7.67 (d, *J* = 8.3 Hz, 1H), 7.62 (s, 1H), 7.24 (d, *J* = 9.3 Hz, 1H), 5.64 (s, 1H), 4.60-4.51 (m, 1H), 4.20 – 4.09 (m, 2H), 2.94 – 2.73 (m, 5H), 2.47 (s, 3H, CH_3), 2.34 (s, 1H), 2.15-1.94 (m, 4H), 1.90 – 1.63 (m, 6H), 1.55 – 1.40 (m, 3H), 1.35 (s, 3H, CH_3), 1.29 (d, *J* = 1.7 Hz, 2H), 1.26 (t, J = 6.9 Hz, 3H, CH_3), 1.19 (s, 1H), 1.14 (s, 6H, 2×CH_3), 1.11 (s, 3H, CH_3), 1.04 – 0.96 (m, 2H), 0.84 (d, *J* = 6.6 Hz, 6H, 2×CH_3), 0.80 (s, 3H, CH_3), 0.76 (s, 1H). ^{13}C NMR (75

MHz, $CDCl_3$) δ 199.99, 176.36, 172.03, 170.14, 169.34, 158.16, 145.93, 133.95, 132.17, 128.44, 127.75, 121.29, 120.19, 81.51, 61.68, 60.29, 55.04, 48.41, 45.38, 43.83, 43.21, 41.08, 38.75, 38.08, 37.71, 36.93, 32.68, 31.81, 31.21, 31.12, 29.76, 29.23, 28.54, 28.28, 28.03, 26.43, 23.52, 23.31, 21.42, 18.67, 17.34, 16.64, 16.34, 14.30. HR-MS (m/z) (ESI): calcd for $C_{44}H_{60}N_2O_6S$ [M+H^+]: 745.42503; found: 745.42519.

18β-3-O-(β-(4'-methoxylbenzothiazolyl)amidepropionyl)-11-oxo-olean-12-en-30-oic acid ethyl ester ***(11d)***. This was obtained as a light yellow solid (62 mg, 82%). ^{1}H NMR (500 MHz, $CDCl_3$) δ 8.44 (d, *J* = 8.5 Hz, 1H, NH), 7.98 (s, 1H), 7.14 – 7.11 (m, 1H), 7.04 (d, *J* = 1.9 Hz, 1H), 5.64 (s, 1H), 4.59 – 4.52 (m, 1H), 4.22 – 4.10 (m, 2H), 3.93 (s, 3H, OCH_3), 2.83 – 2.78 (m, 1H), 2.77 – 2.70 (m, 4H), 2.35 (s, 1H), 2.13 – 1.90 (m, 4H), 1.87 – 1.62 (m, 6H), 1.49 – 1.38 (m, 3H), 1.36 (s, 3H, CH_3), 1.34 – 1.29 (m, 2H), 1.26 (t, J = 6.9 Hz, 3H, CH_3), 1.23 – 1.17 (m, 1H), 1.14 (d, *J* = 4.1 Hz, 6H, 2×CH_3), 1.12 (s, 3H, CH_3), 1.06 – 1.00 (m, 2H), 0.87 (d, *J* = 1.3 Hz, 6H, 2×CH_3), 0.80 (s, 3H, CH_3), 0.78 (s, 1H). ^{13}C NMR (125 MHz, $CDCl_3$) δ 199.96, 176.33, 172.36, 169.82, 169.35, 148.58, 148.52, 129.60, 128.44, 124.51, 120.56, 117.14, 112.48, 81.33, 61.70, 60.28, 56.15, 55.08, 48.41, 45.39, 43.83, 43.23, 41.10, 38.77, 38.10, 37.72, 36.95, 32.70, 32.53, 31.81, 31.12, 29.71, 28.54, 28.28, 28.06, 26.49, 26.43, 23.55, 23.32, 18.68, 17.37, 16.66, 16.34, 14.30. HR-MS (m/z) (ESI): calcd for $C_{44}H_{61}N_2O_7S$ [M+H^+]: 761.41995; found: 761.42302.

18β-3-O-(β-(6'-methoxylbenzothiazolyl)amidepropionyl)-11-oxo-olean-12-en-30-oic acid ethyl ester ***(11e)***. This was obtained as a light yellow solid (59 mg, 77%). ^{1}H NMR (300 MHz, $CDCl_3$) δ 11.07 (s, 1H, NH), 7.68 (d, *J* = 8.9 Hz, 1H), 7.30 (d, *J* = 2.5 Hz, 1H), 7.05 – 7.00 (m, 1H), 5.64 (s, 1H), 4.59 – 4.52 (m, 1H), 4.21 – 4.11 (m, 2H), 3.87 (s, 3H, OCH_3), 2.85 – 2.79 (m, 1H), 2.79 (s, 4H), 2.34 (s, 1H), 2.15 – 1.93 (m, 4H), 1.88 – 1.62 (m, 6H), 1.53 – 1.38 (m, 3H), 1.35 (s, 3H, CH_3), 1.34 – 1.29 (m, 2H), 1.26 (t, J = 6.9 Hz, 3H, CH_3), 1.22 – 1.17 (m, 1H), 1.14 (s, 6H, 2×CH_3), 1.11 (s, 3H, CH_3), 1.04 – 0.97 (m, 2H), 0.85 (d, *J* = 6.1 Hz, 6H, 2×CH_3), 0.80 (s, 3H, CH_3), 0.76 (s, 1H). ^{13}C NMR (75 MHz, $CDCl_3$) δ 199.99, 176.36, 172.08, 170.03, 169.35, 156.92, 156.84, 142.20, 133.29, 128.44, 121.24, 115.28, 104.39, 81.52, 61.68, 60.29, 55.83, 55.04, 48.41, 45.38, 43.83, 43.22, 41.08, 38.75, 38.08, 37.71, 36.93, 32.68, 31.81, 31.18, 31.13, 29.25, 28.54, 28.28, 28.04, 26.48, 26.43, 23.52, 23.31, 18.67, 17.35, 16.65, 16.34, 14.30. HR-MS (m/z) (ESI): calcd for $C_{44}H_{61}N_2O_7S$ [M+H^+]: 761.41995; found: 761.42057.

*18β-3-O-(β-(4'-fluorobenzothiazolyl)amidepropionyl)-11-oxo-olean-12-en-30-oic acid ethyl ester (**11f**).* This was obtained as a light yellow solid (54 mg, 72%). ^{1}H NMR (500 MHz, $CDCl_3$) δ 11.13 (s, 1H, NH), 7.63 (d, *J* = 8.0 Hz, 1H), 7.31 – 7.28 (m, 1H), 7.21 – 7.16 (m, 1H), 5.68 (s, 1H), 4.60-4.56 (m, 1H), 4.24 – 4.15 (m, 2H), 2.87 (s, 1H), 2.86 – 2.81 (m, 4H), 2.38 (s, 1H), 2.17 – 2.00 (m, 4H), 1.88 – 1.66 (m, 6H), 1.53-1.43 (m, 3H), 1.39 (s, 3H, CH_3), 1.35 (d, *J* = 8.3 Hz, 2H), 1.30 (t, J = 6.9 Hz, 3H, CH_3), 1.27 – 1.22 (m, 1H), 1.18 (s, 6H, 2×CH_3), 1.15 (s, 3H, CH_3), 1.05 (d, *J* = 13.2 Hz, 2H), 0.89 (s, 3H, CH_3), 0.87 (s, 3H, CH_3), 0.84 (s, 3H, CH_3), 0.81 (s, 1H). ^{13}C NMR (125 MHz, $CDCl_3$) δ 199.97, 176.36, 171.91, 170.51, 169.33, 159.25, 155.51, 136.77, 134.90, 128.46, 124.62, 117.20, 112.13, 111.99, 81.49, 61.69, 60.30, 55.04, 48.42, 45.39, 43.84, 43.23, 41.10, 38.75, 38.08, 37.73, 36.94, 32.70, 31.82, 31.14, 30.99, 29.23, 28.54, 28.29, 28.04, 26.50, 26.44, 23.50, 23.32, 18.69, 17.36, 16.63, 16.34, 14.30. HR-MS (m/z) (ESI): calcd for $C_{43}H_{58}FN_2O_6S$ [M+H$^+$]: 749.39996; found: 749.40005.

*18β-3-O-(β-(6'-fluorobenzothiazolyl)amidepropionyl)-11-oxo-olean-12-en-30-oic acid ethyl ester (**11g**).* This was obtained as a light yellow solid (63 mg, 84%). ^{1}H NMR (500 MHz, $CDCl_3$) δ 10.70 (s, 1H, NH), 7.74-7.69 (m, 1H), 7.50 (dd, *J* = 8.0, 2.4 Hz, 1H), 7.15 (td, *J* = 8.9, 2.5 Hz, 1H), 5.65 (s, 1H), 4.60-4.54 (m, 1H), 4.20 – 4.10 (m, 2H), 2.83-2.81 (m, 1H), 2.81-2.77 (m, 4H), 2.35 (s, 1H), 2.14-1.92 (m, 4H), 1.86-1.63 (m, 6H), 1.53-1.38 (m, 3H), 1.35 (s, 3H, CH_3), 1.34-1.30 (m, 2H), 1.26 (t, J = 6.9 Hz, 3H, CH_3), 1.23-1.17 (m, 1H), 1.14 (s, 6H, 2×CH_3), 1.12 (s, 3H, CH_3), 1.06-0.99 (m, 2H), 0.86 (d, *J* = 5.2 Hz, 6H, 2×CH_3), 0.80 (s, 3H, CH_3), 0.77 (s, 1H). ^{13}C NMR (126 MHz, $CDCl_3$) δ 199.98, 176.36, 172.22, 170.18, 169.39, 160.60, 144.63, 128.45, 121.69, 126.61, 114.70, 114.51, 107.84, 107.63, 81.72, 61.69, 60.30, 55.06, 48.42, 45.39, 43.84, 43.24, 41.11, 38.77, 38.11, 37.73, 36.95, 32.70, 31.82, 31.25, 31.14, 29.24, 28.55, 28.28, 28.06, 26.50, 26.44, 23.56, 23.31, 18.69, 17.37, 16.67, 16.35, 14.30. HR-MS (m/z) (ESI): calcd for $C_{43}H_{58}FN_2O_6S$ [M+H$^+$]: 749.39996; found: 749.39950.

*18β-3-O-(β-(4'-chlorobenzothiazolyl)amidepropionyl)-11-oxo-olean-12-en-30-oic acid ethyl ester (**11h**).* This was obtained as a light yellow solid (60 mg, 79%). ^{1}H NMR (500 MHz, $CDCl_3$) δ 10.68 (s, 1H, NH), 7.78 (d, *J* = 1.9 Hz, 1H), 7.69 (d, *J* = 8.6 Hz, 1H), 7.38 (dd, *J* = 8.6, 2.0 Hz, 1H), 5.65 (s, 1H), 4.60 – 4.55(m, 1H), 4.19 – 4.11 (m, 2H), 2.84 – 2.81 (m, 1H), 2.80 (s, 4H), 2.34 (s, 1H), 2.14 – 1.95 (m, 4H), 1.89 – 1.63 (m, 6H), 1.45 – 1.38 (m, 3H), 1.35 (s, 3H, CH_3), 1.32 – 1.30 (m, 2H), 1.26 (t, J = 6.9 Hz, 3H, CH_3), 1.22 – 1.17 (m, 1H), 1.14 (s, 6H, 2×CH_3), 1.12 (s, 3H,

CH_3), 1.04 – 0.99 (m, 2H), 0.86 (d, *J* = 5.6 Hz, 6H, 2×CH_3), 0.80 (s, 3H, CH_3), 0.77 (s, 1H). ^{13}C NMR (125 MHz, $CDCl_3$) δ 199.97, 176.35, 172.22, 170.24, 169.38, 158.72, 146.83, 133.44, 129.47, 128.45, 126.94, 121.61, 121.07, 81.75, 61.69, 60.29, 55.06, 48.42, 45.39, 43.83, 43.23, 41.10, 38.77, 38.11, 37.72, 36.95, 32.70, 31.82, 31.27, 31.14, 29.23, 28.55, 28.28, 28.06, 26.50, 26.44, 23.56, 23.32, 18.69, 17.36, 16.66, 16.36, 14.30. HR-MS (m/z) (ESI): calcd for $C_{43}H_{58}ClN_2O_6S$ [M+H^+]: 765.37041; found: 765.37037.

*18β-3-O-(β-(6'-chlorobenzothiazolyl)amidepropionyl)-11-oxo-olean-12-en-30-oic acid ethyl ester (**11i**)*. This was obtained as a light yellow solid (63 mg, 82%). ^{1}H NMR (500 MHz, $CDCl_3$) δ 10.60 (s, 1H, NH), 7.78 (d, *J* = 2.0 Hz, 1H), 7.69 (d, *J* = 8.6 Hz, 1H), 7.38 (dd, *J* = 8.6, 2.0 Hz, 1H), 5.65 (s, 1H), 4.59 – 4.53 (m, 1H), 4.19 – 4.12 (m, 2H), 2.83 – 2.81 (s, 1H), 2.80 (s, 4H), 2.35 (s, 1H), 2.13 – 1.98 (m, 4H), 1.93 – 1.67 (m, 6H), 1.53 – 1.40 (m, 3H), 1.35 (s, 3H), 1.34 – 1.30 (m, 2H), 1.26 (t, J = 6.9 Hz, 3H), 1.23 – 1.18 (m, 1H), 1.14 (s, 6H, 2×CH_3), 1.12 (s, 3H), 1.06 – 1.01 (m, 2H), 0.86 (d, *J* = 5.2 Hz, 6H, 2×CH_3), 0.80 (s, 3H), 0.77 (s, 1H). ^{13}C NMR (125 MHz, $CDCl_3$) δ 199.97, 176.35, 172.23, 170.23, 169.39, 158.63, 146.85, 133.45, 129.46, 128.45, 126.93, 121.64, 121.06, 81.76, 61.70, 60.30, 55.06, 48.42, 45.39, 43.84, 43.24, 41.11, 38.77, 38.12, 37.73, 36.95, 32.70, 31.82, 31.29, 31.14, 29.24, 28.55, 28.29, 28.06, 26.50, 26.44, 23.56, 23.32, 18.69, 17.37, 16.67, 16.36, 14.30. HR-MS (m/z) (ESI): calcd for $C_{43}H_{58}ClN_2O_6S$ [M+H^+]: 765.37041; found: 765.36987.

*18β-3-O-(β-(4'-bromobenzothiazolyl)amidepropionyl)-11-oxo-olean-12-en-30-oic acid ethyl ester (**11j**)*. This was obtained as a light yellow solid (67 mg, 83%). ^{1}H NMR (500 MHz, $CDCl_3$) δ 10.18 (s, 1H, NH), 7.75 (d, *J* = 7.9 Hz, 1H), 7.62 (d, *J* = 7.8 Hz, 1H), 7.16 (t, *J* = 7.9 Hz, 1H), 5.64 (s, 1H), 4.58 – 4.52 (m, 1H), 4.20 – 4.11 (m, 2H), 2.83 – 2.78 (m, 5H), 2.35 (s, 1H), 2.15 – 1.92 (m, 4H), 1.87 – 1.62 (m, 6H), 1.55 – 1.40 (m, 3H), 1.35 (s, 3H, CH_3), 1.34-1.29 (m, 2H), 1.26 (t, J = 6.9 Hz, 3H, CH_3), 1.22 – 1.17 (m, 1H), 1.14 (s, 6H, 2×CH_3), 1.12 (s, 3H, CH_3), 1.05 – 1.00 (m, 2H), 0.85 (d, *J* = 9.4 Hz, 6H, 2×CH_3), 0.80 (s, 3H, CH_3), 0.77 (s, 1H). ^{13}C NMR (125 MHz, $CDCl_3$) δ 199.97, 176.37, 171.86, 170.19, 169.35, 158.41, 146.71, 133.05, 129.64, 128.45, 124.83, 120.64, 114.44, 81.57, 61.69, 60.31, 55.04, 48.42, 45.39, 43.84, 43.23, 41.10, 38.75, 38.10, 37.72, 36.95, 32.70, 31.82, 31.27, 31.14, 29.19, 28.55, 28.29, 28.06, 26.50, 26.44, 23.53, 23.33, 18.69, 17.36, 16.68, 16.35, 14.30. HR-MS (m/z) (ESI): calcd for $C_{43}H_{58}BrN_2O_6S$ [M+H^+]: 811.31990; found: 811.31766.

*18β-3-O-(β-(6′-bromobenzothiazolyl)amidepropionyl)-11-oxo-olean-12-en-30-oic acid ethyl ester (**11k**).* This was obtained as a light yellow solid (56 mg, 69%). ^{1}H NMR (500 MHz, $CDCl_3$) δ 10.63 (s, 1H, NH), 7.93 (d, *J* = 1.8 Hz, 1H), 7.64 (d, *J* = 8.6 Hz, 1H), 7.51 (dd, *J* = 8.6, 1.8 Hz, 1H), 5.65 (s, 1H), 4.60 – 4.54(m, 1H), 4.20 – 4.11 (m, 2H), 2.82 (s, 1H), 2.80 (s, 4H), 2.35 (s, 1H), 2.14 – 1.94 (m, 4H), 1.90-1.64 (m, 6H), 1.54 – 1.39 (m, 3H), 1.35 (s, 3H, CH_3), 1.34 – 1.30 (m, 2H), 1.26 (t, J = 6.9 Hz, 3H, CH_3), 1.23 – 1.18 (m, 1H), 1.14 (s, 6H, 2×CH_3), 1.12 (s, 3H, CH_3), 1.05 – 1.00 (m, 2H), 0.86 (d, *J* = 5.3 Hz, 6H, 2×CH_3), 0.80 (s, 3H, CH_3), 0.77 (s, 1H). ^{13}C NMR (125 MHz, $CDCl_3$) δ 199.98, 176.35, 172.23, 170.25, 169.39, 158.69, 147.18, 133.92, 129.66, 128.45, 123.97, 122.02, 116.89, 81.77, 61.70, 60.30, 55.06, 48.42, 45.40, 43.84, 43.24, 41.11, 38.77, 38.12, 37.73, 36.95, 32.70, 31.82, 31.29, 31.14, 29.23, 28.55, 28.29, 28.07, 26.50, 26.44, 23.56, 23.32, 18.69, 17.37, 16.67, 16.37, 14.30. HR-MS (m/z) (ESI): calcd for $C_{43}H_{58}BrN_2O_6S$ [$M+H^+$]: 811.31990; found: 811.31898.

4.3. Hsp90-Cdc37 disruption measurement.

The HTRF experiments were conducted in 384-well black low volume plate (Greiner#784076) in PBS buffer (containing 400 mM KF, pH = 7.3). For each assay, 4 μL His-tagged full-length Hsp90 (250 nM finial) and 4 μL GST-tagged $Cdc37_M$ (250 nM finial) were mixed into the plate wells. Then 4 μL diluted compounds were added and mixed. After incubated at 37 ^{o}C for 1 h, 4 μL anti-GST-Cryptate (61GSTKLA, CISBIO) and 4 μL anti-6His-XL665 (61HISXLA, CISBIO) were added and incubated at 37 ^{o}C for additional 0.5 h. Then the time-resolved fluorescence was measured using Molecular Device (SpectraMax paradigm; excitation = 320 nm, emissions = 665 nm and 620 nm). The HTRF ratio was calculated as a two-wavelength signal ratio: (Signal 665 nm/Signal 620 nm)×10,000. Negative control (His-Hsp90, GST-Cdc37M, anti-GST-Cryptate, anti-6His-XL665) and blank control (anti-6His-XL665 and anti-GST-Cryptate) were conducted for each assay. Data analysis was conducted by using Graphpad Prim 6.0 software.

4.4. Molecular docking.

All the docking studies were carried out using Sybyl-X 2.0 on a windows workstation. The crystal structure of the Hsp90-Cdc37 complex were retrieved from the RCSB Protein Data Bank (PDB: 1US7).[41] The synthetic analogues **6**, **7**, and **11** were selected for the docking studies. The 3D structures of these selected compounds were first built using Sybyl-X 2.0 sketch followed by energy minimization using the MMFF94 force field and Gasteiger-Marsili charges. We employed

Powell's method for optimizing the geometry with a distance dependent dielectric constant and a termination energy gradient of 0.005 kcal/mol. All the selected compounds were automatically docked into the binding pocket of Hsp90—Cdc37 by an empirical scoring function and a patented search engine in the Surflex docking program. Before the docking process, the natural ligand was extracted; the water molecules were removed from the crystal structure. Subsequently, the protein was prepared by using the Biopolymer module implemented in Sybyl. The polar hydrogen atoms were added. The automated docking manner was applied in the present work. Other parameters were established by default to estimate the binding affinity characterized by the Surflex-Dock scores in the software. Surflex-Dock total scores, which were expressed in -log10 (Kd) units to represent binding affinities, were applied to estimate the ligand-receptor interactions of newly designed molecules. A higher score represents stronger binding affinity. The optimal binding pose of the docked compounds was selected based on the Surflex scores and visual inspection of the docked complexes.

4.5. Cell culture and maintenance.

All human cancer cell lines and human normal liver cells in this study were purchased from China Life Science Collage (Shanghai, PRC). Culture medium Dulbecco's modified Eagle medium (DMEM), fetal bovine serum (FBS), phosphate buffered saline (PBS, pH=7.2), and Antibiotice-Antimycotic came from KeyGen Biotech Company (China). Cell lines were grown in the supplemented with 10% FBS, 100 units/ml of penicillin and 100 g/ml of streptomycin in a humidified atmosphere of 5% CO_2 at 37 ^{o}C.

4.6. Cytotoxicity assay.

The anticancer activity of the target compounds were dissolved in DMSO and evaluated in four human cancer cells (A549, MCF-7, HepG2, Hct-116, and NCI-H460) and DOX-resistance cells (NCI-H460/DOX), respectively. About 1.0×10^5 cells/mL cells, which were in the logarithmic phase, were grown in each well of 96-well plates and incubated for 12 h at 37 °C in 5% CO_2. The tested compounds at five different concentrations (2.5, 5, 10, 20 and 50 μM) were also added to the test well and then the cells were incubated at 37 °C in a 5% CO_2 atmosphere for 48 h. An enzyme labeling instrument was used to read absorbance with 570/630 nm double wavelength measurement. Cytotoxicity was detected on the percentage of cell survival compared with the negative control. The final IC_{50} values were calculated by the Bliss method (n = 5). All of the tests

were repeated in triplicate.

4.7. Flow cytometry analysis of cell cycle distribution.

A549 cells were grown on 6-well plates and treated with compound **11g** at the indicated concentrations (5 and 10 μM) and maintained with of the proper culture medium in 5% CO_2 at 37 ℃ for 48 h. The untreated cells were served as negative control. After completion of incubation, cells were harvested and washed three times with ice-cold PBS, fixed with ice-cold 70% ethanol at -20 ℃ for overnight. The cells were treated with 100 μg /mL RNase A for 30 minutes at 37 ℃ after washed with twice ice-cold PBS, and finally stained with 1 mg/ml propidium iodide (PI) in the dark at 4 ℃ for 30 minutes. Analysis was performed with the system software (Cell Quest; BD Biosciences).

4.8. Apoptosis analysis.

Apoptosis was also investigated by flow cytometric analysis of annexin V/PI staining. A549 cells were grown in each well of six-well plates at the density of 1.0×10^5 cells/mL of the DMEM medium with 10% FBS to the final volume of 2 mL. The plates were incubated for overnight and treated with **11g** at the indicated concentrations (5 and 10 μM) for 24 h. Briefly, cells were harvested and washed with twice ice-cold PBS, and then suspended cells in the annexin-binding buffer at a concentration of 5×10^5 cells /ml. cells were then incubated with 5 μL of annexin V-FITC and 5 μL of PI in the dark at 4 ℃ for 30 minutes. The cells were detected by system software (Cell Quest; BD Biosciences).

4.9. Hoechest33258 staining.

The Hoechst 33258 molecular probes were also used to investigate apoptotic cells. A549 cells (5.0×10^5 cells) were grown in six-well tissue culture plates and treated with compound **11g** at the indicated concentrations (5 and 10 μM) for 24 h and untreated cells were served as negative control. Then the cells were fixed in 4% paraformaldehyde for 30 minutes followed by the medium was discarded. Cells were then washed twice with ice-cold PBS and incubated with 0.5 mL of Hoechst 33258 at dark for 20 minutes. After for 30 minutes incubation, cells were washed twice with ice-cold PBS and the results were analysis by a Nikon ECLIPSETE2000-S fluorescence microscope using 350 nm excitation and 460 nm emissions.

4.10. ROS assay.

The production of ROS was examined by flow cytometry using DCFH-DA. A549 cells were

seeded into six-well plates and subjected to various treatments. On the following treatment, cells were collected at 2000 rpm and washed twice with ice-cold PBS, and then resuspend cells in 10mM DCFH-DA dissolved in cell free medium at 37 ℃ for 20 minutes in dark, and then washed twice with ice-cold PBS. Cellular fluorescence was analyzed by flow cytometry at an excitation of 485 nm and an emission of 538 nm.

4.11. Western blot analysis.

A549 cells were treated with the tested compound **11g** at the indicated concentrations (5 and 10 μM) for 24 h. After that time, cells were harvested, centrifuged, and washed twice with ice-cold PBS. The pellet was then resuspended in lysis buffer. After the cells were lysed on ice for 20 min, lysates were centrifuged at 20000g at 4 ℃ for 5 min. The protein concentration in the supernatant was analyzed using the BCA protein assay reagents (Imgenex, USA). Equal amounts of protein per line were was separated on 12% SDS polyacrylamide gel electrophoresis and transferred to PVDF Hybond-P membrane (GE Healthcare). Membranes were incubated with 5% skim milk in Tris-buffered saline with Tween 20 (TBST) buffer for 1 h and then the membranes being gently rotated overnight at 4 °C. Membranes were then incubated with primary antibodies against Bcl-2, Bax, caspase-9, caspase-3, or β-actin for overnight at 4 °C. Membranes were next incubated with peroxidase labeled secondary antibodies for 2 h. Then all membranes were washed with TBST three times for 15 minutes and the protein blots were investigated with chemiluminescence reagent (Thermo Fischer Scientifics Ltd.). The X-ray films were developed with developer and fixed with fixer solution.

4.12. Immunoprecipitation

A549 cells were treated with **11g** and geldanamycin at the indicated concentrations (5 and 10 μM) for 24 h. Cells were lysed in 20 mM Tris HCl (pH 7.4), 25 mM NaCl, 2 mM DDT, 20 mM Na_2MoO_4, 0.1% NP-40, and protein inhibitors. Lysates were incubated for 2 h at 4°C, rotating, and then centrifuged at 13,000×g for 10 min. Protein (500 μg) was incubated with anti-HSP90 antibody overnight at 4°C, rotating. Protein G agarose (30 μl) was added to each sample, and samples were then incubated for 1 h at 4°C, rotating. The beads were washed five times with 1 ml lysis buffer. Bound proteins were isolated by boiling in sample buffer. The levels of HSP90 and coimmunoprecipitating proteins were analyzed by western blot.

4.13. Statistical analysis.

All statistical analysis was performed with SPSS Version 10. Data was analyzed by one-way ANOVA. Mean separations were performed using the least significant difference method. Each experiment was replicated thrice, and all experiments yielded similar results. Measurements from all the replicates were combined, and treatment effects were analyzed.

Acknowledgements

This research was financially supported by National Key Basic Research Program of China (grant No. 2013CB933904), by Natural Science Foundation of China (Grant Nos. 81671745, 21431001 and 81760626), by Industry Project of Jiangsu Science-technology Support Plan (grant No. BE2013840), by Science and Technology Development Program of Suzhou (grant No. ZXY201412).

A. Supplementary data

Supplementary data associated with this article can be found, in the online version, at

References

1. Fidler J, Kripke ML. Metastasis results from preexisting variant cells within a malignant tumor. *Science*. 1997;197:893-895.
2. Szakács G, Paterson JK, Ludwig JA, et al. Targeting multidrug resistance in cancer. *Nat Rev Drug Discov.* 2006;5:219-34.
3. Kim MK, Kim Y, Choo H, et al. Quercetin-glutamic acid conjugate with a non-hydrolysable linker; a novel scaffold for multidrug resistance reversal agents through inhibition of P-glycoprotein. *Bioorg Med Chem*. 2016;25:1219-1226
4. Jiang F, Wang HJ, Jin YH, et al. Novel Tetrahydropyrido[4,3-d]pyrimidines as Potent Inhibitors of Chaperone Heat Shock Protein 90. *J Med Chem.* 2016;59:10498-10519.
5. Qin JM, Huang RZ, Yao GY, et al. Terminal functionalized thiourea-containing dipeptides as multidrug-resistance reversers that target 20S proteasome and cell proliferation. *Eur J Med Chem*. 2017;126:259-269.
6. Yao F, Wang G, Wei W, et al. An autophagy inhibitor enhances the inhibition of cell proliferation. *Mol Med Rep*. 2012;5:84-88.
7. Gong J, Luk F, Jaiswal R, et al. Microparticle drug sequestration provides a parallel pathway in the acquisition of cancer drug resistance. *Eur J Pharmacol.* 2013;721:116-125.

8. Whitesell L, Lindquist SL. Hsp90 and the chaperoning of cancer. *Nat Rev Cancer.* 2005;5:761-772.
9. Vo CD, Shebert HL, Zikovich S, et al. Repurposing Hsp90 inhibitors as antibiotics targeting histidine kinases. *Bioorg Med Chem Lett*. 2017;27:5235-5244.
10. Bhat R, Tummalapalli SR, Rotella DP. Progress in the discovery and development of heat shock protein 90 (Hsp90) inhibitors. *J Med Chem*. 2014;57:8718-8728.
11. Taddei M, Ferrini S, Giannotti L, et al. Synthesis and evaluation of new Hsp90 inhibitors based on a 1,4,5-trisubstituted 1,2,3-triazole scaffold. *J Med Chem*. 2014;57:2258-2274.
12. Shao LD, Su J, Ye B, et al. Design, synthesis, and biological activities of vibsanin B derivatives: a new class of HSP90 C-terminal inhibitors. *J Med Chem*. 2017;60:9053-9066.
13. Huang W, Ye M, Zhang LR, et al. FW-04−806 inhibits proliferation and induces apoptosis in human breast cancer cells by binding to N-terminus of Hsp90 and disrupting Hsp90-Cdc37 complex formation. *Mol Cancer.* 2014;13:150-163.
14. Wang MN, Shen AJ, Zhang C, et al. Development of heat shock protein (Hsp90) inhibitors to combat resistance to tyrosine kinase inhibitors through Hsp90−kinase interactions. *J Med Chem*. 2016;59:5563-5586.
15. Li DR, Li C, Li L, et al. Natural product kongensin a is a non-canonical Hsp90 inhibitor that blocks RIP3-dependent necroptosis. *Cell Chem Biol*. 2016;23:257-266.
16. Wang L, Li L, Zhou ZH, et al. Structure-based virtual screening and optimization of modulators targeting Hsp90-Cdc37 interaction. *Eur J Med Chem.* 2017;136:63-73.
17. Vaughan CK, Mollapour M, Smith JR, et al. Hsp90-dependent activation of protein kinases is regulated by chaperone-targeted dephosphorylation of Cdc37. *Mol Cell.* 2008;31:886-895.
18. Schwarze SR, Fu VX, Jarrard DF. Cdc37 enhances proliferation and is necessary for normal human prostate epithelial cell survival. *Cancer Res.* 2003;63:4614–4619.
19. Smith JR, Workman P. Targeting CDC37: An alternative, kinase-directed strategy for disruption of oncogenic chaperoning. *Cell Cycle*. 2009;8:362-372.
20. Zhang T, Hamza A, Cao X, et al. A novel Hsp90 inhibitor to disrupt Hsp90/Cdc37 complex against pancreatic cancer cells. *Mol Cancer Ther*. 2008;7:162-170.

21. He J, Ning C, Wang Y, et al. Natural plant flavonoid apigenin directly disrupts Hsp90/Cdc37 complex and inhibits pancreatic cancer cell growth and migration. *J Functional oods*. 2015;18:10-21.
22. Brandt GEL, Schmidt MD, Prisinzano TE, et al. Gedunin, a Novel Hsp90 Inhibitor: Semisynthesis of Derivatives and Preliminary Structure−Activity Relationships. *J Med Chem*. 2008;51:6495-6502.
23. Zhang T, Hamza A, Cao X, et al. A novel Hsp90 inhibitor to disrupt Hsp90/Cdc37 complex against pancreatic cancer cells. *Mol Cancer Ther*. 2008;7:162-170.
24. Zou LW, Li YG, Wang P, et al. Design, synthesis, and structure-activity relationship study of glycyrrhetinic acid derivatives as potent and selective inhibitors against human carboxylesterase 2. *Eur J Med Chem*. 2016;112:280-288.
25. Parida PK, Sau A, Ghosh T, et al. Synthesis and evaluation of triazole linked glycosylated 18β-glycyrrhetinic acid derivatives as anticancer agents. *Bioorg Med Chem Lett.* 2014;24:3865-3868.
26. Li K, Ma TY, Cai JJ, et al. Conjugates of 18b-glycyrrhetinic acid derivatives with 3-(1H-benzo[d] imidazol-2-yl)propanoic acid as Pin1 inhibitors displaying anti-prostate cancer ability. *Bioorg Med Chem.* 2017;25:5441-5451.
27. Liu D, Song D, Guo G, et al. The synthesis of 18β-glycyrrhetinic acid derivatives which have increased antiproliferative and apoptotic effects in leukemia cells. *Bioorg Med Chem.* 2007; 15:5432-5439.
28. Noolvi MN, Patel HM, Kaur M. Benzothiazoles: search for anticancer agents. *Eur J Med Chem*. 2012;54:447-462.
29. Vasconcelos TRA, Gomes CRB, Reis RDR, et al. Chemistry and Biological Activities of 1,3-Benzothiazoles. *Mini Rev Org Chem*. 2012;9:44-53.
30. Rao AVS, Swapna K, Shaik SP, et al. Synthesis and biological evaluation of cis-restricted triazole/tetrazole mimics of combretastatin-benzothiazole hybrids as tubulin polymerization inhibitors and apoptosis inducers. *Bioorg Med Chem*. 2016;25:977-999.
31. Kamal A, Mallareddy MJ, Ramaiah SNCVL, et al. Synthesis and biological evaluation of combretastatin-amidobenzothiazole conjugates as potential anticancer agents. *Eur J Med Chem*. 2012;56:166-178.

32. Lee E, An Y, Kwon J, et al. Optimization and biological evaluation of 2-aminobenzothiazole derivatives as Aurora B kinase inhibitors. *Bioorg Med Chem*. 2017;25:3614-362
33. Guo W, Yan M, Xu B, et al. Design, synthesis, and biological evaluation of the novel glycyrrhetinic acid-cinnamoyl hybrids as anti-tumor agents. *Chem Cent J*. 2016;10:78-89.
34. Leblanc V, Delaunay V, Claude LF, et al. Homogeneous time-resolved fluorescence assay for identifying p53 interactions with its protein partners, directly in a cellular extract. *Anal Biochem*. 2002;308:247-254.
35. Shen S, Zhou M, Huang K, et al. Blocking autophagy enhances the apoptotic effect of 18β-glycyrrhetinic acid on human sarcoma cells via endoplasmic reticulum stress and JNK activation. *Cell Death Dis*. 2017;8:e3055.
36. Xiao L, Rasouli P, Ruden DM. Possible effects of early treatments of hsp90 inhibitors on preventing the evolution of drug resistance to other anti-cancer drugs. *Curr Med Chem*. 2007;14:223-232.
37. Huang RZ, Liang GB, Huang XC, et al. Discovery of dehydroabietic acid sulfonamide based derivatives as selective matrix metalloproteinases inactivators that inhibit cell migration and proliferation. *Eur J Med Chem*. 2017;138:979-992.
38. Memmel S, Sisario D, Zöller C, et al. Migration pattern, actin cytoskeleton organization and response to PI3K-, mTOR-, and Hsp90-inhibition of glioblastoma cells with different invasive capacities. *Oncotarget*. 2017;8:45298-45310.
39. Simon HU, Haj-Yehia A, Levi-Schaffer F, Role of reactive oxygen species (ROS) in apoptosis induction. *Apoptosis*. 2000;5;415-418.
40. Qu HE, Huang RZ, Yao GY, et al. Synthesis and pharmacological evaluation of novel bisindole derivatives bearing oximes moiety: Identification of novel proapoptotic agents. *Eur J Med Chem*. 2015;95:400-415.
41. Dispersyn G, Nuydens R, Connors R, et al. Bcl-2 protects against FCCP-induced apoptosis and mitochondrial membrane potential depolarization in PC12 cells. *Biochimica Et Biophysica Acta-General Subjects*. 1999;1428:357-371.
42. Cook SA, Sugden PH, Clerk A. Regulation of Bcl-2 family proteins during development and in response to oxidative stress in cardiac myocytes. *Circ Res*. 1999;85:940-949.

43. Kluck RM, Bossy-Wetzel E, Green DR, et al. The release of cytochrome c from mitochondria: a primary site for Bcl-2 regulation of apoptosis. *Science*. 1997;275:1132-1136.

44. Shan M, Fan TJ. Cytotoxicity of carteolol to human corneal epithelial cells by inducing apoptosis via triggering the Bcl-2 family protein-mediated mitochondrial pro-apoptotic pathway. *Toxicol In Vitro*. 2016;35:36-42.

45. Liu X, Zhang Y, Huang W, et al. Design, synthesis and pharmacological evaluation of new acyl sulfonamides as potent and selective Bcl-2 inhibitors. *Bioorg Med Chem*. 2018;26:443-454.

46. Roe SM, Ali MMU, Meyer P, et al. The mechanism of Hsp90 regulation by the protein kinase-specific cochaperone p50(Cdc37). *Cell*. 2004;116:87-98.

Graphical abstract

Discovery of 18β-glycyrrhetinic acid conjugated aminobenzothiazole derivatives as Hsp90–Cdc37 interaction disruptors that inhibit cell migration and reverse drug resistance

Le Jin, Rizhen Huang, Xiaochao Huang, Bin Zhang, Min Ji and Hengshan Wang

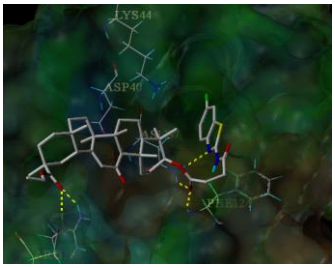

Disrupt Hsp90-Cdc37 interaction

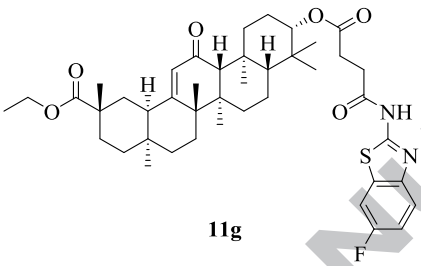

11g

Inhibit cell proliferation

Reverse drug resistance

Suppress cell migration

Induce apoptosis

Arrest cell cycle

Highlights

- A novel series of 18β-glycyrrhetinic acid (GA) conjugated aminobenzothiazole derivatives were synthesized.
- Compound **11g** disrupted the interaction of Hsp90-Cdc37.
- Molecular modeling suggested that **11g** tightly binds to the active site of Hsp90-Cdc37 complex.
- The inhibitors efficiently reversed drug-resistant and inhibited the cell migration of human lung cancer cells.
- **11g** induced apoptosis and arrested cell cycle at S phase in A549 cells.